

UTAH
SEVIER
CITY OF MONROE
ne ne 280 fml 268 fel.

3 MC

15-25s-3w
HOT SPRINGS

GD

1500 test. El: 5500 GR.
Contr: Sweetwater Drlg. Spud 3/15/79. 16 @ 650, 7 5/8 liner 600-1300.
1971 TD. Comp 4/6/79. IPF 280 gal/min @ 164° F. Prod Zone: faulted Volcanics
1300-1471 (open hole).

UT1-022980

 **Petroleum Information.**
CORPORATION
A Subsidiary of E. I. du Pont de Nemours & Co.

© COPYRIGHTED 1979
REPRODUCTION PROHIBITED Form No. 611

GLB1534

UTAH
SEVIER
CITY OF MONROE
ne ne 280 fnl 268 fel.

3 MC

15-25s-3w
HOT SPRINGS

GD

1500 test. El: 5500 GR.
Contr: Sweetwater Drlg. Spud 3/15/79. 16 @ 650, 7 5/8 liner 600-1300.
1971 TD. Comp 4/6/79. IPF 280 gal/min @ 164° F. Prod Zone: faulted Volcanics
1300-1471 (open hole).

UT1-022980

 **Petroleum Information.**
CORPORATION
A Subsidiary of A.C. Nielsen Company

© COPYRIGHTED 1979
REPRODUCTION PROHIBITED Form No. 611

SEVIER CO

PI

No

✓148 ○ 36.4 °C/hm

✓150 ○

UGMS

No.

✓1 ○

✓2 ○

✓3 ○

✓4 ○

✓5 ○

✓6 △

✓7 ○ 35.6 °C/hm

✓8 ○

SEVIER

TOTAL ALL WELLS 10

" ANOMALOUS " 2

Sec	T	R	d	BHT	GRAD	AMB
2	24S	4E	1191 m	52.2°C	36	8.9
8	25S	4E	1216 m	52.2°C	36	8.9

FORCED CONVECTIVE HEAT TRANSFER IN THE MONROE HOT SPRINGS GEOTHERMAL SYSTEM

KEVIN KILTY, DAVID S. CHAPMAN and CHARLES W. MASE

Department of Geology and Geophysics, University of Utah, Salt Lake City, UT 84112 (U.S.A.)

(Received August 15, 1978; revised and accepted February 23, 1979)

ABSTRACT

Kilty, K., Chapman, D.S. and Mase, C.W., 1979. Forced convective heat transfer in the Monroe hot springs geothermal system. *J. Volcanol. Geotherm. Res.*, 6: 257-277.

A knowledge of convective heat transfer is essential to understanding geothermal systems and other systems of moving groundwater. A simple, kinematic approach toward convective heat transfer is taken in this paper. Concern is not with the cause of the groundwater motion but only with the fact that the water is moving and transferring heat.

The mathematical basis of convective heat transfer is the energy equation which is a statement of the first law of thermodynamics. The general solution of this equation for a specific model of groundwater flow has to be done numerically. The numerical algorithm used here employs a finite difference approximation to the energy equation that uses central differences for the heat conduction terms and one-sided differences for the heat convection terms. Gauss-Seidel iteration is then used to solve the finite difference equation at each node of a non-uniform mesh.

The Monroe and Red Hill hot springs, a small hydrothermal system in central Utah, provide an example to illustrate the application of convective heat transfer theory to a geophysical problem. Two important conclusions regarding small geothermal systems follow immediately from the results of this application. First, the most rapid temperature rise in the convecting part of a geothermal system is near the surface. Below this initially rapid temperature increase the temperature increases very slowly, and thus temperatures extrapolated from shallow boreholes can be seriously in error. Second, the temperatures and heat flows observed at Monroe and Red Hill, and probably at many other small geothermal areas, can easily result from moderate vertical groundwater velocities in faults and fracture zones in an area of normal heat flow.

INTRODUCTION

Convective heat transfer, the process in which heat is transferred by a moving medium such as groundwater, is common in geological situations. Geysers and hot springs are spectacular examples. More pervasive however is ordinary groundwater flow which at velocities of the order of 10^{-8} m/s transfers as much heat as conduction. Understanding convective heat transfer is therefore important in studying the thermal regime in many regions of the upper crust particularly in geothermal areas where convection is the dominant heat transfer process.

The recent interest in geothermal energy has led to an increased study of convective heat transfer in geothermal problems (Sorey, 1975; Lowell, 1975; Bodvarsson, 1969). Yet much of the work on geothermal systems is not completely satisfactory. For example, Blackwell and Chapman (1977) have successfully modelled a fault-controlled geothermal system. However, instead of treating the convective heat transfer rigorously they used isothermal planes to represent the groundwater flow. Under what conditions is this a valid approximation?

Rigorous treatments of convective heat transfer also have several shortcomings. First there is a preoccupation with free convection — convection driven by thermal buoyancy. While free convection is important in systems with powerful heat sources, other systems it may not be nearly as important as forced convection. Furthermore, the fluid flow and heat transfer in free convection problems depend strongly on the geometry and permeability of the system and the heat source which are poorly known in geological situations.

In this paper we examine numerical models of heat transfer and their application to the Monroe—Red Hill geothermal system in central Utah. In our modeling we have taken a kinematic standpoint, being concerned more with heat transfer than fluid dynamics, since we constrain our models with temperature and heat flow data. Beyond simply presenting the results for Monroe—Red Hill we wish to broaden into a general discussion of heat transfer and our mathematical model of it. Because the Monroe—Red Hill system is similar to many geothermal systems that are fault controlled we feel a general discussion of our model and the theory behind it may be useful for studies elsewhere.

MATHEMATICAL AND CONCEPTUAL MODELS

The mathematical analysis of any heat transfer problem involves solving the energy equation, so called because it describes conservation of energy, for the boundary conditions and groundwater velocity field appropriate to the problem. The time-dependent form of this equation is (Stallman, 1963):

$$\nabla \cdot K_c \nabla T - C_f \rho_f (\vec{V} \cdot \nabla T) = C_c \rho_c \frac{\partial T}{\partial t} \quad (1)$$

where K_c , C_c , ρ_c are the thermal conductivity, specific heat and density of the solid-fluid composite material, C_f and ρ_f are the specific heat and density of the fluid, \vec{V} is the velocity field of the fluid averaged over a representative volume of material, T is the temperature, and t is time.

The validity of this equation depends on two conditions. First, it is valid only if the divergence of the velocity field, $(\nabla \cdot \vec{V})$, and viscous dissipation are negligible. These restrictions are generally met in steady groundwater flow. Second, it is strictly valid only if the solid and fluid phases can both be regarded as continua. Of course this restriction can never be satisfied exactly since the fluid phase can only exist in pore spaces where no solid phase is

present. However, it is approximately satisfied if the pore spaces and fractures through which the flow takes place are smaller than the distance over which there is a significant temperature change. A significant temperature change may be 0.01°C or 1.0°C depending on the nature of the problem. If these restrictions are not met the energy equation contains additional terms. Singh and Dybbs (1974) and Slattery (1972) discuss the form of these additional terms.

The factor that most complicates the solution of the energy equation is the groundwater velocity field, \vec{V} . In forced convection problems the velocity field is primarily the result of external pressures and can be determined independently of the temperature field. For small velocities the relationship between the velocity field and external pressures is given by Darcy's law (Davis and DeWiest, 1966)

$$\vec{V} = -K_h \nabla \varphi \quad (2)$$

where φ is the force potential as defined by Hubbert (1940), and K_h is the hydraulic conductivity of the solid which in general may be a second rank tensor, but is treated as a constant scalar here.

The hydraulic conductivity is a combined property of the solid and the fluid. It is related to permeability which is a property of the solid alone according to the equation

$$K_h = k \frac{\gamma}{\mu} \quad (3)$$

where k is permeability, γ is the specific weight of the fluid, and μ is the dynamic viscosity of the fluid.

Free convection problems are more complicated because the velocity field is primarily the result of thermal buoyancy; or equivalently stated, the force potential is a function of temperature. Darcy's law as stated above is valid for free convection problems if the concept of force potential is modified to include the equation of state for a fluid (Elder, 1965):

$$\rho(T) = \rho_0 [1 - \alpha(T - T_0)] \quad (4)$$

where ρ_0 is the density at a temperature equal to T_0 , and α is the volume expansion coefficient; and:

$$\varphi = \int_{P_0}^P \frac{dP'}{\rho} + \int_{z_0}^z g [1 - \alpha(T - T_0)] dz' \quad (5)$$

where P is the hydrostatic pressure at a height of z , and P_0 is the hydrostatic pressure on a reference datum z_0 .

Since Darcy's law and the energy equation in free convection problems both depend on temperature, these equations have to be solved simultaneously. In order to avoid the difficulty of solving coupled differential equations we neglect free convection and consider only forced convection in the remainder of this paper.

QUALITATIVE ASPECTS OF HEAT TRANSFER

If the quantities L_0 , V_0 , t_0 , T_0 and T_s are respectively a characteristic length, velocity, time, temperature, and surface temperature in a convective flow, the transformations $\nabla^* = L_0 \nabla$, $\vec{V}^* = \vec{V}/V_0$, $t^* = t/t_0$, and $\theta = (T - T_s)/(T_0 - T_s)$ result in a dimensionless energy equation (Slattery, 1972):

$$\frac{1}{N_{Pe}} \nabla^{*2} \theta - (\vec{V}^* \cdot \nabla^* \theta) = \frac{R}{N_{St}} \frac{\partial}{\partial t^*} \theta \quad (6)$$

The characteristic quantities may be chosen arbitrarily as long as they are chosen the same in problems with similar geometry (Rosenberger, 1978).

The dimensionless energy equation contains three dimensionless groups of parameters; R , N_{St} , and N_{Pe} . R is the ratio of the heat capacity of the solid-fluid composite, $C_c \rho_c$, to the heat capacity of the fluid, $C_f \rho_f$. N_{St} is the Strouhal number defined as $N_{St} = V_0 t_0 / L_0$. If t_0 is chosen to be the characteristic time for thermal conduction, L_0^2 / α_c (where α_c is the thermal diffusivity), the Strouhal number is the ratio of the time required for thermal diffusion to the time required for thermal convection (Le Mehaute, 1976). The Strouhal number also determines how time is measured (Luikov, 1966).

N_{Pe} is the Peclet number defined as $N_{Pe} = \rho_f C_f V_0 L_0 / K_c$. It is the ratio of heat transferred by convection to that transferred by conduction in the bulk fluid flow (Rosenberger, 1978). If conduction dominates heat transfer the second term of equation (6) is small and the solution of the energy equation is simply a perturbation of the solution for pure conduction in an equivalent geometry. (Domenico and Palciauskas, 1973, used such a perturbation technique to analyze heat transfer in homogeneous, isotropic alluvium.) Furthermore, the time dependence of the problem is controlled by the factor $R N_{Pe} / N_{St}$ which implies that the time required to reach thermal equilibrium is proportional to $\rho_c C_c L_0^2 / K_c$ — the characteristic time for thermal conduction.

Alternatively, if convection dominates the heat transfer the first term of equation (6) is very small, and the time dependence of the temperature field is controlled by the factor R / N_{St} . This implies that the time required to reach equilibrium is proportional to L_0 / V_0 . Moreover, the steady state of temperature field of the problem ($\partial / \partial t^* = 0$) is described by the equation:

$$\vec{V}^* \cdot \nabla^* \theta = 0$$

The only realistic solution of this equation is θ equal to a constant throughout the bulk fluid flow (Rosenberger, 1978).

NUMERICAL SOLUTION OF THE ENERGY EQUATION

Although a qualitative discussion of the energy equation demonstrates the character of convective heat transfer the analysis of a real geothermal system requires a solution to the equation for a specific flow field. Unfortunately

analytic solutions cannot be obtained except for the simplest situations. In the general case a numerical solution must be sought.

Using the vector identity $\nabla \cdot \alpha \vec{A} = \alpha \nabla \cdot \vec{A} + \nabla \alpha \cdot \vec{A}$ the energy equation (1) can be cast in the form:

$$K_c \nabla^2 T + (\nabla K_c - C_f \rho_f \vec{V}) \cdot \nabla T = C_c \rho_c \frac{\partial T}{\partial t} \quad (7)$$

where all the variables have been defined previously. We use a finite difference solution to this equation that was originally suggested by Courant et al. (1952) and developed in Gosman et al. (1969). This solution uses central differences to approximate the second-order partial derivatives and uses forward or backward differences oriented into the fluid flow to approximate the first-order partial derivatives. The resulting difference equation written at each node of a finite difference grid results in a system of equations that can be solved with iterative methods (Gerald, 1970).

We have organized the numerical algorithm to accept arbitrary groundwater flows, thermal conductivities, and boundary conditions. It also uses a non-uniform grid which can be used to obtain detailed information in the central part of the mesh while removing the disturbing effect of the boundaries as far as possible by expanding the mesh near them.

The accuracy and rate of convergence of the algorithm is strongly dependent on the type of boundary conditions that are used. Constant temperature boundaries provide the most rapid convergence but are not always realistic. A constant flux boundary condition is a better approximation to the lower boundary and sometimes for the vertical boundaries also. The upper boundary, which is the air-ground interface, is best represented by a mixed boundary condition expressed mathematically as:

$$H(T_s - T_a) = K_c \left. \frac{\partial T}{\partial Z} \right|_{Z=0}$$

$(T_s - T_a)$ is the difference between the surface temperature and the ambient air temperature, and H is a semi-empirical film coefficient between the ground surface and the air. This boundary condition frees the surface from an isothermal state and allows phenomena such as warm or steaming ground to evolve naturally in the simulations.

An approximate value of the film coefficient can be determined from boundary layer theory by knowing the mean wind speed in the area (Chapman, 1974). However, estimating the film coefficient from wind speeds is not completely satisfactory because it assumes that the heat transfer between the earth and air occurs by conduction through a stagnant film of air. The actual heat transfer mechanism is probably transfer of water vapor to the air in evapo-transpiration (Sophocleous, personal communication). We have used values of 0.3–1.2 $\text{W m}^{-2} \text{K}^{-1}$ for the film coefficient with a value of 0.6 $\text{W m}^{-2} \text{K}^{-1}$ giving the most reasonable results.

At large groundwater velocities ($N_{Pe} > 200$) the truncation error of the

one-sided differences leads to a fictitious diffusion (Gosman et al., 1969) which degrades the accuracy of the solution. The effect of fictitious diffusion is best discussed by referring to the dimensionless energy equation (6). At large Peclet numbers the time-dependent form of this equation is approximately:

$$\vec{V}^* \cdot \nabla^* \theta = - \frac{R}{N_{St}} \frac{\partial \theta}{\partial t^*}$$

This is a hyperbolic differential equation much like those used to describe shock waves. Thus, at large Peclet numbers large thermal gradients (thermal shocks) develop near boundaries or rapid changes in groundwater velocity. Fictitious diffusion smooths these sharp temperature changes.

The magnitude of the fictitious diffusion is proportional to $|V|h \sin 2\alpha$, where $|V|$ is the absolute value of the groundwater velocity, h is the spacing of the finite difference nodes, and α is the angle between the streamlines and the finite difference net (Gosman et al., 1969). In geophysical problems h is generally quite large (> 50 m) so that the fictitious diffusion may be substantial even for small groundwater velocities.

Two ways of reducing the effect of fictitious diffusion are to use a fine finite difference net (small h) or a finite difference net that parallels the streamlines of the flow. Gosman et al. (1969) discuss this in more detail.

MODEL OF A FAULT-CONTROLLED GEOTHERMAL SYSTEM

The discussion, which so far has been very general, is now narrowed to a particular geophysical problem — that of heat transfer in a fault-controlled geothermal system. Fig. 1 shows a simple model of the system.

The thermal water originates as surface water that percolates down through faults, fractures, and aquifers into a storage area beneath the hot springs. During the downward percolation and during its residence time in the storage area the water absorbs heat from its surroundings. Eventually it is forced from the storage area through a fault zone to a discharge area at the surface. At the surface part of the water discharges through the hot spring while the remainder is lost through leakage to the alluvium. The location of the hot spring is determined by the piezometric surface, topography, and the location of a permeable conduit in the fault zone.

The pressure that forces the water to the surface is supplied principally by the difference in elevation between the recharge and discharge areas; although buoyancy over heat sources could supply some additional pressure. Once the discharge is started a further contribution to the driving pressure is derived from the temperature difference between the discharging and recharging water columns. Simon (1960) noted this driving pressure in a Hungarian artesian well which, after being shut in for one day, had cooled enough to stop flowing and had to be restarted by pumping.

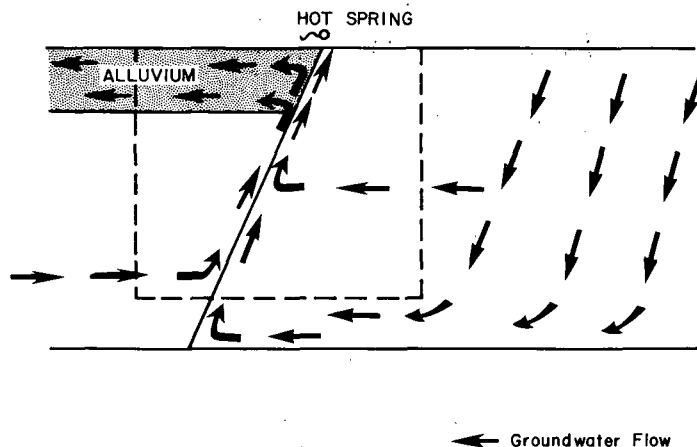


Fig. 1. Simple model of a fault-controlled geothermal system. The thermal water originates from surface water that recharges a deep reservoir and absorbs heat in the process. It is eventually forced up the fault zone, mixes with other water at various levels, and leaks into the alluvium or discharges at the surface.

An interesting way of applying convective heat transfer theory to this model follows an approach often used in fluid mechanics problems. In fluid mechanics the solutions to many problems are empirical relations, determined experimentally or numerically, between a determining criterion such as the velocity of a specific flow field and a non-determining criterion such as the heat or momentum that is transferred. These relationships are most useful if the comparison is between dimensionless criteria (Luikov, 1966).

In heat transfer problems the determining criteria are the dimensionless coordinates and the Peclet and Strouhal numbers. The non-determining criteria are the dimensionless temperature and the Nusselt number, $N_{Nu} = L_0 \partial \theta / \partial z|_{z=0}$, which is the ratio of total heat transfer at the surface to the heat that would be transferred by conduction alone (Luikov, 1966). An example of a relationship between determining and non-determining criteria in the context of our model (Fig. 1) is illustrated in Fig. 2.

Fig. 2 shows a numerically determined relationship between the Nusselt number at the earth's surface directly over a fracture and the Peclet number of the flow up the fracture. The small inset in the figure shows the geometry of the flow. The flow begins in a reservoir at a depth L_0 and flows up a fracture to a depth of d . L_0 is chosen as the characteristic length in the problem because it is characteristic of the temperature difference between the fluid at depth and the surface. At a depth of d the flow becomes predominantly horizontal as the fluid moves toward small conduits to discharge at the surface.

Not surprisingly the figure shows the Nusselt number to be a monotonically increasing function of Peclet number. As the Peclet number approaches

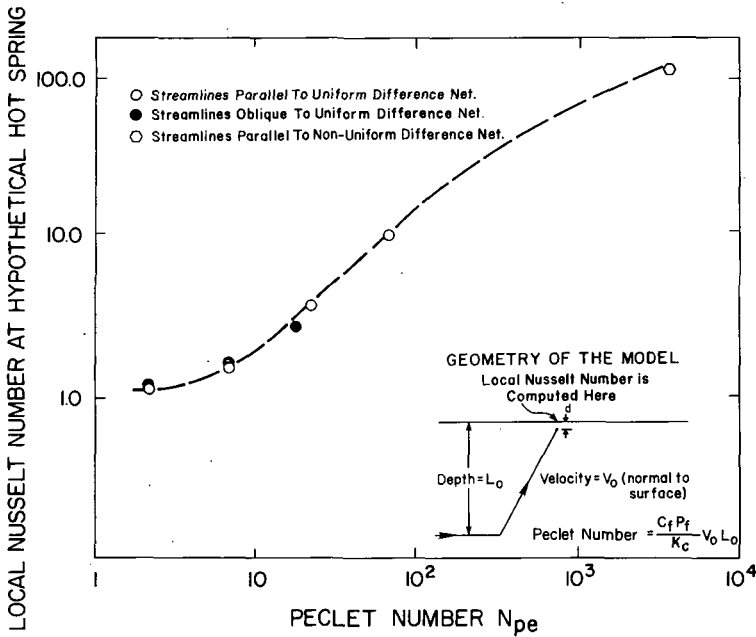


Fig. 2. Relationship between the heat-flow enhancement (Nusselt number) directly over a fracture and the Peclet number of the flow up the fracture for the geometry shown in the inset.

zero ($V_0 \rightarrow 0$) the Nusselt number asymptotically approaches a value of unity—characteristic of pure conduction. Alternatively, as the Peclet number becomes very large the Nusselt number approaches a limiting value of L_0/d —characteristic of fluid moved instantaneously from a depth L_0 to d (Jaeger, 1965). Fig. 2 was calculated with L_0/d equal to 200; therefore, the Nusselt number is approaching the value 200.

A figure like Fig. 2 is useful for inverting heat-flow measurements to obtain the velocity of the groundwater flow up any similar fracture geometry. Once the Nusselt number is determined from a heat-flow measurement over the fracture the relationship of Fig. 2 fixes the Peclet number or the value of the product $V_0 L_0$ for the flow.

Many other relationships between determining and non-determining criteria are possible. For instance, Jaffrennou et al. (1974) experimentally determined a relationship between Nusselt number and filtration Rayleigh number in free convection and Sorey (1975) numerically determined a relationship between the dimensionless drop in water temperature between the reservoir and hot spring and the dimensionless discharge of the hot spring. The relationships that are most useful, of course, depend on the nature of the specific problem.

APPLICATION TO THE MONROE, UTAH, HYDROTHERMAL SYSTEM

The Monroe and Red Hill hot springs are located on the east side of the central Sevier Valley near Monroe, Utah. They issue from the Sevier fault which is a major, west-dipping normal fault that separates the Tertiary volcanic rocks of the Sevier Plateau from the alluvium of the Sevier Valley.

The first detailed studies of these hot springs (Parry et al., 1976; Miller, 1976) were concerned with the geochemistry and alteration mineralogy of the systems and provide valuable constraints on the origin and history of the thermal waters. During the autumn of 1976 and throughout 1977, geophysical surveys including precision gravity, ground-magnetics, and dipole-dipole electric soundings were conducted and a borehole drilling program was undertaken to provide direct subsurface temperature information (Halliday, 1978; Mase, 1978).

Hydrogeology

The hydrogeologic situation in the central Sevier Valley is shown in Fig. 3. The geologic and hydrologic information in the figure is generalized from Young and Carpenter (1965), Hahl and Mundorff (1968), and Stokes and Hintze (1963).

The subsurface hydrology of the central Sevier Valley is very complex. This is partially because of complicated geological structure and partially because of the number of aquifers that could contribute to the subsurface flow. The Sevier Plateau and the Pavant Range southwest of the town of Richfield are covered with up to 4 km of Oligocene and Pliocene volcanic rocks (Young and Carpenter, 1965). The volcanic rocks consist of pyroclastic rocks in the lowest part overlain by latite flows which are, in turn, overlain by basaltic andesite flows, rhyolite, and tuffs. Young and Carpenter (1965) indicate that these volcanic rocks generally have very low permeabilities. The pyroclastic rocks, tuffs, and latite flows surely have low permeability but the basaltic andesite flows are locally very permeable as shown by springs that discharge from them. Moreover, all of the volcanic rocks have higher permeabilities in the fractured and faulted zones.

The volcanic rocks lie upon sedimentary rocks that range in age from Oligocene to Jurassic, depending on location. The silty and shaly sequences, such as the Jurassic Arapien shale, have low permeability but many of the sandstones and limestones, such as the Jurassic Navajo sandstone and the Tertiary Flagstaff limestone, are very permeable and make good aquifers (Young and Carpenter, 1965). These aquifers outcrop in the Tushar Mountains southwest of Marysvale and they also outcrop extensively in the Pavant Range west of Richfield where they dip to the south and southeast under the volcanic rocks (Callaghan and Parker, 1961). Their structure under the volcanic rocks is unknown. The Mesozoic and older sedimentary rocks are folded and thrust-faulted (Hardy, 1952) and all of the rocks, including

the volcanic rocks, were faulted and fractured during Basin and Range normal faulting which began during Miocene times and has continued sporadically to the present.

The recharge of the sedimentary aquifers occurs in the mountainous areas which receive 75 cm of water or more per year as precipitation. The aquifers can recharge directly from surface precipitation wherever they outcrop; otherwise their recharge depends on available fractures and faults in the over-

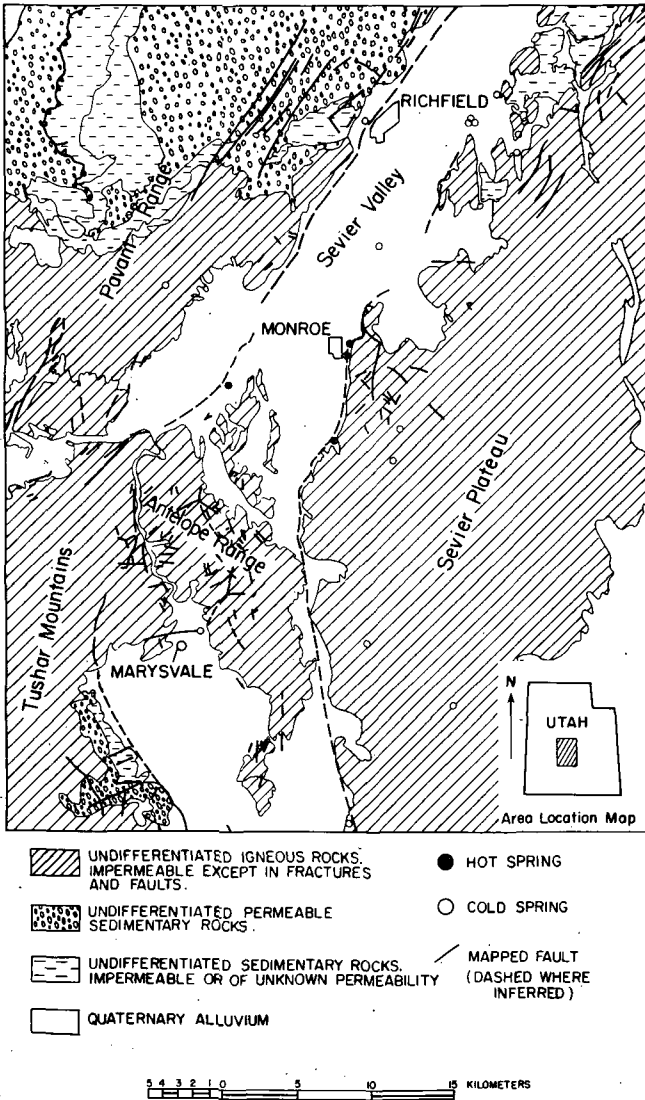


Fig. 3. Generalized hydrogeology in the area around Monroe Hot Springs, Utah.

lying volcanic rocks. Once the groundwater has infiltrated these aquifers it may move laterally into reservoirs deep beneath the valley floor.

The valley floor is formed of narrow, down-dropped fault blocks covered with Pliocene and Pleistocene sediments which vary in thickness from a thin veneer to as much as 500 meters (Young and Carpenter, 1965). The fill lies upon an unknown thickness of volcanic rocks which isolate it from the deeper, sedimentary aquifers. The fill is composed of fanglomerates, clays, landslide deposits, and terrace and streambed gravels. This heterogeneous composition causes the permeability of the fill to vary from good to poor.

The hot springs

Hot springs occur in well-defined seeps on the Sevier fault at Monroe, Red Hill, and Johnson warm spring. The springs occur at changes in the trend of the surface trace of the Sevier fault. Perhaps these are the only locations where the fault zone is permeable enough for the water to penetrate the surface. Hot water may rise from depth in many other places along the fault only to mix with cool water and leak into the alluvium before it can discharge at the surface.

Mase (1978) has drawn inferences about the near-surface hot spring discharge from the first separation dipole-dipole apparent resistivity shown in Fig. 4. The contours generally follow the Sevier fault as located by the ground magnetic survey (Mase, 1978) and close on the hottest and most altered part of the system. The 5 Ω -m contours probably outline conduits up which the hot springs fluid 30% porous saturated sediments would have an apparent that at the temperature ($\sim 70^\circ\text{C}$) and salinity (3800 ppm NaCl equiv.) of the hot springs fluid 30% porous saturated sediments would have an apparent resistivity of 5 Ω -m (Keller and Frischnecht, 1966).

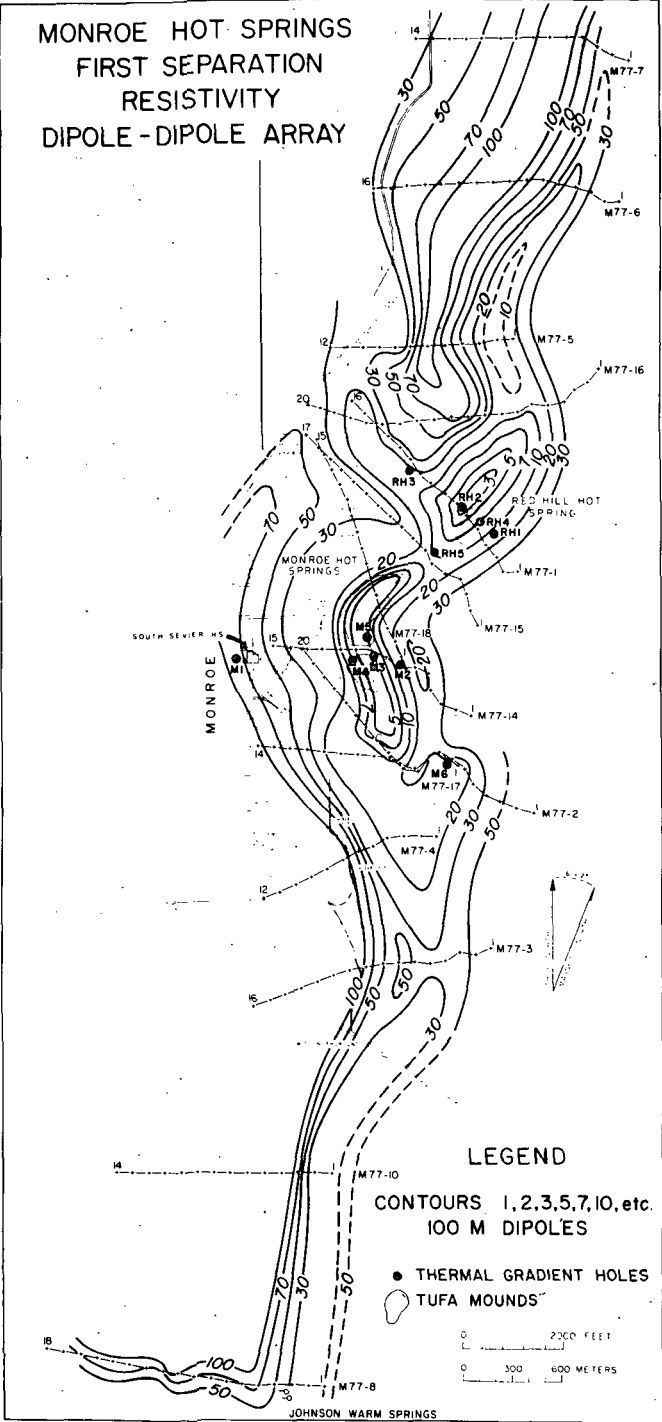
Once the hot springs fluid cools to 25–30°C the sediments containing it would have an apparent resistivity of 15–10 Ω -m. On this basis the arm of low resistivity projecting northwest from Red Hill probably represents the leakage of cooling thermal fluids through the alluvium. A similar leakage zone is indicated extending westward from Johnson Warm springs.

Another important aspect of Fig. 4 is that it shows the predominant two-dimensional geometry of the system and justifies using two-dimensional models to analyze it.

Subsurface temperature data

Mase (1978) obtained direct subsurface temperature data in 11 boreholes, the positions of which are indicated on the insets in Figs. 5 and 7 with the temperature-depth curves. The appearance of the temperature-depth curves is similar to those that Lachenbruch et al. (1976) describe at Long Valley, California and those that Smith (1970) describes at Broadlands, New Zealand.

MONROE HOT SPRINGS FIRST SEPARATION RESISTIVITY DIPOLE - DIPOLE ARRAY



A peculiarity of temperature-depth curves near strongly convecting zones is that the thermal gradient is quite variable with depth, so that making temperature extrapolations on the basis of these curves is risky. The nearly isothermal appearance of two of the boreholes at Red Hill below 30 m depth indicates a strongly convecting zone. The other boreholes at Red Hill and all those at Monroe show a strong, consistent, downward curvature. This curvature may indicate an increase of thermal conductivity with depth, a weak, diffused upward convection, or lateral heat conduction away from a strongly convecting zone. Mase (1978) measured the thermal conductivity in all of the boreholes at 5-m intervals, and found no increase in thermal conductivity with depth. The cause of the curvature is then either upward convection or lateral heat conduction.

An unfortunate aspect of the measurements at Red Hill and Monroe is that none were made away from the immediate area of the hot springs. Such data contain information about the subsurface flow and the location of the recharge area (Lachenbruch et al., 1976).

The temperature data at Monroe and Red Hill are displayed on the east-west cross-sections of Figs. 6 and 8. In each the isotherms are upwarped under the discharge vent and taper off to the east and west. The asymmetry in the isotherms is attributed to several effects, such as the dip of the fault zone through which the hot water is rising, lower thermal conductivity of the alluvium west of the fault, and possible warm-water leakage to the west.

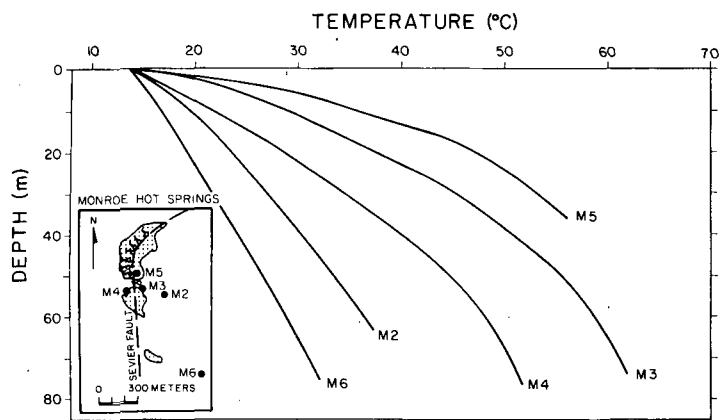


Fig. 5. Temperature-depth curves at Monroe Hot Springs and locations of the various boreholes. The increasing curvature of the temperature-depth curves near the Sevier fault zone shows it to be the locus of the convective heat transfer.

Fig. 4. Contour map depicting first separation dipole-dipole apparent resistivity. The form of the contours indicates the nearly two-dimensional geometry of the system. The locations of eleven heat-flow boreholes are also indicated.

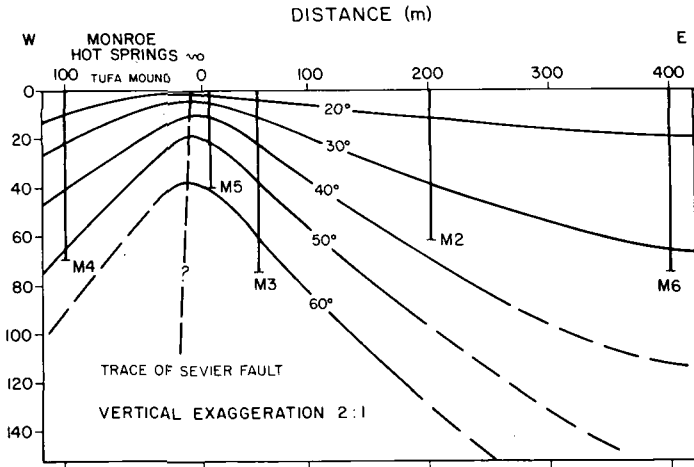


Fig. 6. West-east thermal cross-section at Monroe Hot Springs.

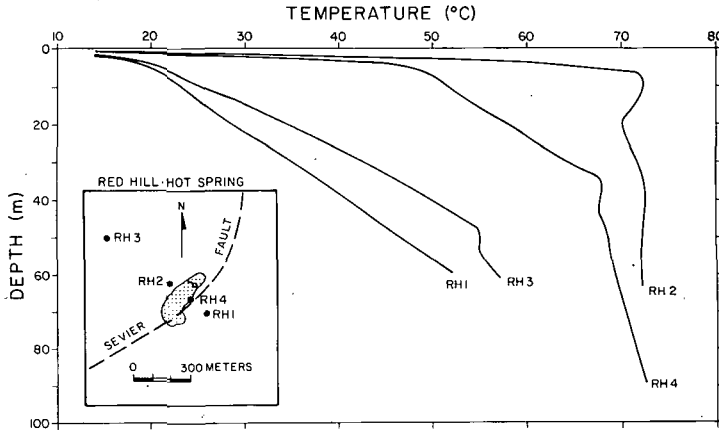


Fig. 7. Temperature-depth curves at Red Hill Hot Spring and the locations of the various boreholes. The nearly isothermal behavior of RH4 and RH2 indicates a strongly convecting zone.

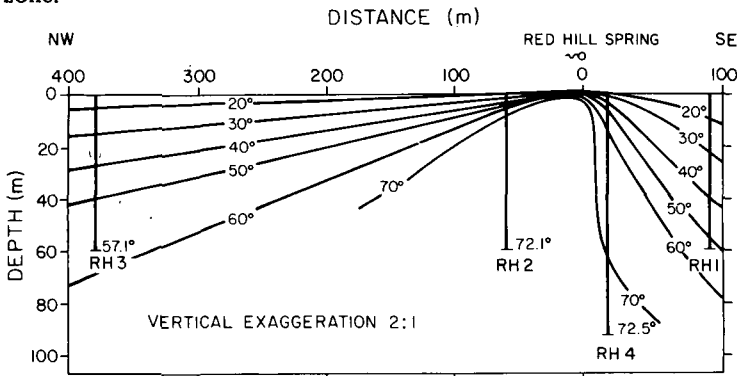


Fig. 8. West-east thermal cross-section of Red Hill Hot Spring.

Geochemical and geophysical constraints

From geochemistry, Parry et al. (1976) determined that the spring waters are most likely a mixture of a hot, saline component and a cool component that is chemically similar to the surface water in the area. A mixing model, based on the measured silica content of the warm water and the warm-water enthalpy, indicated a mixture of 62% hot water at 118°C and 38% cold water at 10°C. The Na-K-Ca geochemistry indicated a hot component temperature of 180°C. In a normal Basin and Range heat-flow area these temperatures are reached between 2.5 and 4.0 km depth. The Na-K-Ca temperature estimate is less reliable than the silica temperature because the hot spring water may have acquired its salinity from evaporites in the Arapien shale. Consequently the hot reservoir is probably nearer a temperature of 118°C than 180°C. What aquifer constitutes the hot fluid reservoir is a matter of speculation, but the most likely possibility is the Jurassic Navajo sandstone because it is generally permeable and probably underlies the Sevier Valley at a depth between 2.5 and 4.0 km (Mase, 1978).

The location of mixing between the hot and cold waters is also speculative. The temperature of the cold springs in the area ranges from about 12 to 20°C. Assuming that the water in the cold springs loses no more than 10°C between depth and the surface (Sorey and Lewis, 1976), the maximum temperature that the cool spring waters attain is about 30°C which implies that this water circulates not deeper than 500 m. This temperature estimate is in apparent conflict with Miller's (1976) geochemical estimates of the maximum subsurface temperature of the cool springs. These estimates, which were based on silica content, ranged from 80°C to over 110°C. There is no satisfactory explanation for this conflict, but part of the problem might be that silica thermometry is not always accurate when applied to cool surface water.

The discharge at the Red Hill spring is about 20 l/s and the combined discharge of all the seeps at Monroe hot springs is about 6 l/s (Mase, 1978). Supposing that the upward flow takes place over an area of 2×10^4 m², which is about the area of the 5 Ω -m contour in Fig. 4, the vertical groundwater velocities required to maintain the discharge range from 2.5×10^{-7} to 1×10^{-6} m/s. These velocities are minimum estimates because the effect of leakage to the alluvium has not been considered.

The permeability of the fault zone is not known. Sorey and Lewis (1976) consider permeabilities of 1 to 10 darcies appropriate values for the fault zones in Long Valley. If an intermediate value of 5 darcies is chosen for the permeable part of the fault zone at Red Hill, a vertical piezometric gradient of 2% is required to account for the spring discharge. This piezometric gradient is equivalent to a 50-m decrease in piezometric head in a 2.5-km rise from the reservoir to the surface. Since the piezometric gradient is the same at Monroe as it is at Red Hill, the lower vertical velocities at Monroe imply a lower permeability in this system.

Heat output of the hot springs

In spite of the limited coverage provided by the eleven borehole heat-flow measurements Mase (1978) managed to calculate the total conductive heat loss using an empirical relationship between heat flow and apparent resistivity. By regressing heat-flow measurements against apparent resistivity he found the relationship:

$$q = 5800 \rho_a^{-0.706}$$

where q is heat flow in mW/m^2 , and ρ_a is apparent resistivity in $\Omega\text{-m}$; to be valid for the Monroe—Red Hill system. Using this formula and the resistivity map of Fig. 4 he calculated the total conductive heat loss of the two systems as 3 MW. He also calculated the heat lost in the springs' discharge as 5 MW using the formula:

$$Q = C\dot{m}\Delta T;$$

where Q is the rate of heat loss, C is the specific heat of water, \dot{m} is the mass discharge rate, and ΔT is the difference between the discharge temperature and the mean air temperature. Adding the conductive and discharge heat losses results in a total heat loss of approximately 8 MW. This is equal to the normal Basin and Range heat flow over a 110-km^2 area.

Wilson and Chapman (1978) observe that recharging groundwater absorbs 30–50% of the heat flow in a recharge area. Thus, heat absorbed over a recharge area of $220\text{--}370\text{ km}^2$ could maintain the observed heat loss at Monroe and Red Hill. This is only about 1/4 of the maximum possible recharge area east, west, and south of the hot springs. In addition to the heat absorbed in a recharge area groundwater also absorbs a substantial amount of heat in lateral flow to the storage reservoir.

W.T. Parry (personal communication) has suggested that exothermal alteration of clays in the hydrothermal system may provide a significant portion of the observed power loss. The power provided by chemical reactions depends on the length of time the system has been active and the extent of the alteration which are not known.

DISCUSSION OF MODEL RESULTS

The numerical algorithm was used to compute the temperature distributions of several models of the subsurface flow. Fig. 9 shows the steady-state temperature field resulting from a flow of 1×10^{-6} m/s up a vertical fault. The flow originated at a depth of 2.0 km and it was assumed that no water leaked from the fault zone but that mixing with cool water occurred between 400 and 500 m depth. The steady-state spring temperature in the model was 81°C compared to 74°C measured at Red Hill. An important aspect of this model is that in the strongly convecting part the temperature increases rapidly with depth near the surface but increases very slowly at greater depths.

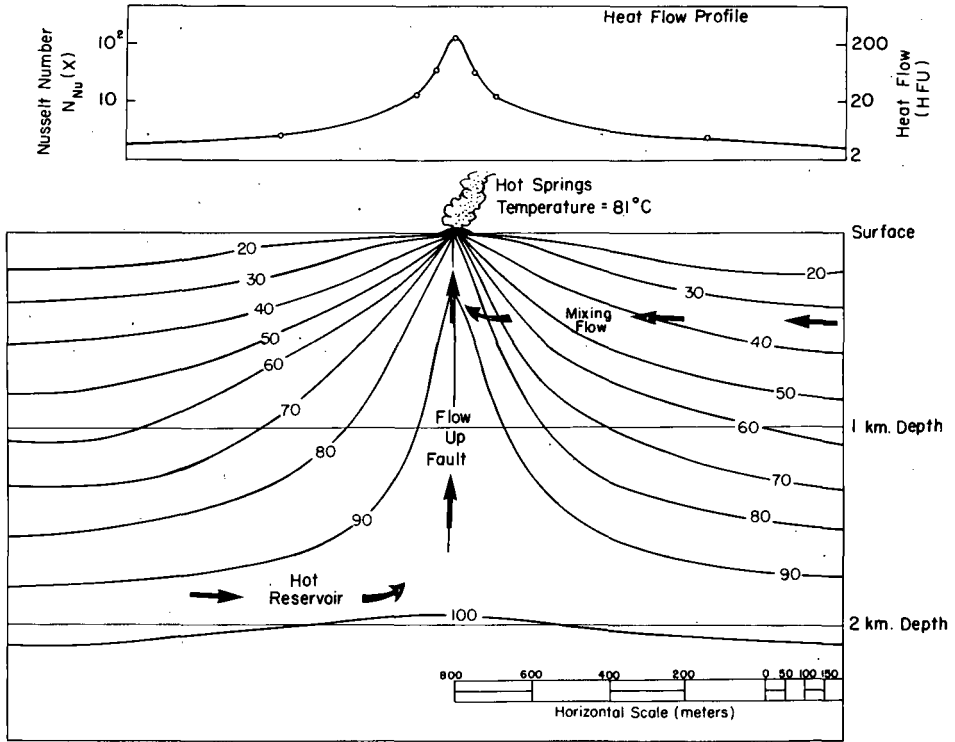


Fig. 9. West-east thermal cross-section through a hypothetical geothermal system. The small mixing flow produces a slight asymmetry to the isotherms. The heat-flow profile, across the system shows a maximum enhancement of $N_{Nu} = 100$. Heat-flow values (HFU) correspond to a 2-HFU background heat flow.

Fig. 10 is a comparison of the observed heat flow at Monroe and Red Hill with two models of the subsurface flow. The axes in the figure are normalized distance from the hot spring perpendicular to the strike of the fault and normalized Nusselt number. The distance is normalized by dividing by the depth at which the flow originated and the Nusselt number is normalized by dividing by the Nusselt number directly over the fracture. In each model the thermal water flows up a vertical fracture from a reservoir at a depth of 2.0 km and the surface discharge is fixed at 0.05 l/s per meter width. In one model all of the flow from the reservoir discharges at the surface while in the other model a fraction of the flow leaks into the alluvium in a 500-m-thick zone. Curves for the cases of 60% and 90% leakage are shown. The observations at Red Hill and Monroe both agree with the models very closely east of the hot springs. West of the hot springs, however, the measurements at the two hot springs are not in agreement each following a different model curve.

At Monroe hot springs the measurements are consistent with a hot springs

discharge through a nearly vertical zone without any leakage to the alluvium. The sharpness of the heat flow anomaly at Monroe indicates that the width of this zone is only about 50 m. A similar geometry, but with a substantial leakage to the alluvium, is consistent with the measurements at Red Hill; thus confirming the interpretation of a leakage zone from the resistivity contour map (Fig. 4).

Although the interpretation has thus far assumed flow in fractures, other interpretations are possible. Fig. 11 illustrates temperature data in borehole M4 compared to temperature-depth curves calculated from two models of the subsurface flow. The observed temperatures in M4 are indistinguishable from the theoretical curve for diffused upward flow. This curve was calculated from a one-dimensional solution of the energy equation assuming a Peclet number of 4.1 and a temperature difference of 45°C between the surface and the subsurface reservoir. This implies that the flow of water is from a 160-m-deep, 60°C reservoir at a rate of $1.2 \times 10^{-8} \text{ s}^{-1}$. While this curve fits the observed data very well, the model it was computed from predicts a terminal temperature of 60°C whereas the hot spring seep nearest M4 has a temperature of 69°C (C.W. Mase, personal communication).

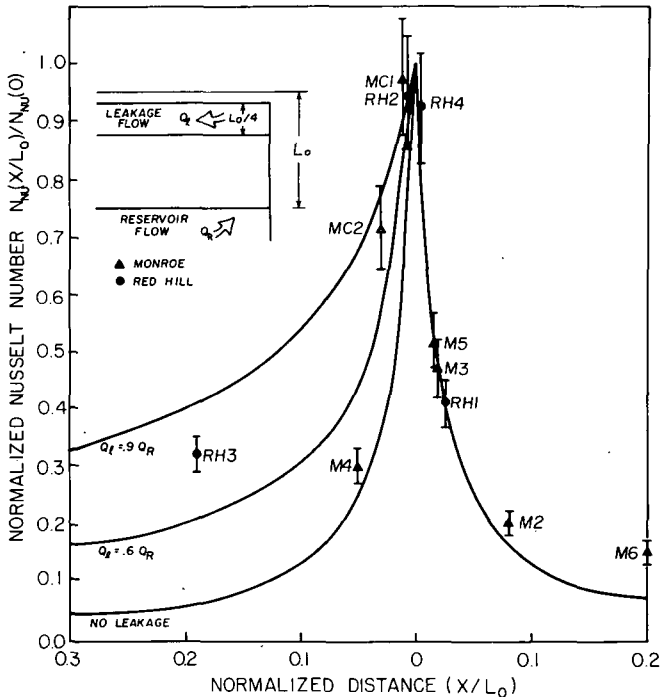


Fig. 10. Numerically determined curves of heat-flow enhancement as a function of distance from the hot spring for the geometry shown. The surface discharge is fixed and the amount of leakage into the alluvium is allowed to vary. Curves for 60% and 90% leakage are shown. Error bars indicate 10% uncertainty in the heat-flow determinations.

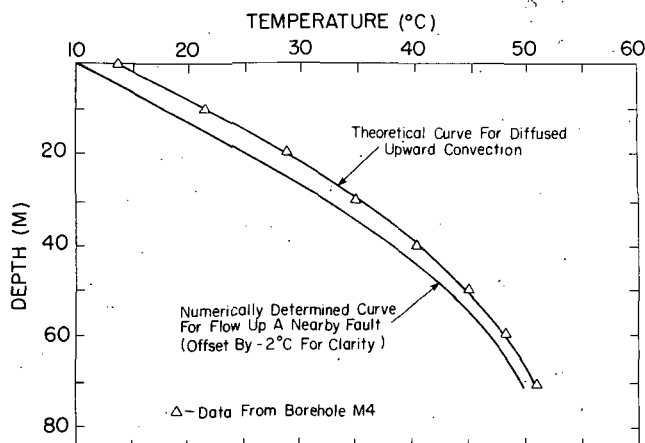


Fig. 11. Temperature data from M4 compared with two temperature-depth curves calculated from different models. While both curves agree well with the data they diverge markedly below 70 m depth where there are no data. Temperature extrapolations depend very much on the model assumed.

The observed data are also consistent with the temperature-depth curve resulting from flow up a 60°-dipping fracture 100 m from the borehole at the surface. This curve was calculated by similarity (Luikov, 1966) with a numerical solution. The interpretation of this curve indicates an upward flow of 1×10^{-7} m/s in the fracture, a local undisturbed geothermal gradient of 400 K/km, and a temperature of 65°C at 120 m depth. Even when constrained by field observations, temperature extrapolations depend very much on the model that is assumed.

IMPLICATIONS FOR MONROE-RED HILL

Temperatures extrapolated to great depths are not generally accurate. However, a prediction based on many models is that the nearly isothermal behavior of two of the boreholes at Red Hill will probably continue until the zone of mixing between the hot and cold components is reached. The temperature could increase 15–20°C within the mixing zone and then continue isothermally to the hot reservoir. The strong downward curvature noted in many of the boreholes likely continues until the maximum reservoir temperature is reached or until a strongly convecting zone is intercepted.

A cooling magma chamber is not necessary as a heat source for the Monroe-Red Hill hydrothermal system. Furthermore, there is no reason to believe that the area has an average heat flow higher than normal for the Basin and Range Province. The following evidence supports these conclusions:

(1) Heat transfer by moving groundwater in a normal Basin and Range heat-flow environment can easily provide the heat loss that is observed at Monroe-Red Hill. Moreover, there may be an additional contribution to the heat flow from exothermic chemical reactions.

(2) There is no indication of Quaternary volcanism in the area.

(3) A piezometric gradient caused by the difference in elevation between recharge areas and the hot spring can maintain the spring's discharge. There is no need for buoyancy over a heat source.

(4) Upward groundwater flow from a reasonably shallow depth of approximately 2.0 km can maintain the temperatures that are observed at Monroe—Red Hill.

The minimum upward velocity that is consistent with the discharge and temperatures at the Red Hill spring is approximately 1×10^{-6} m/s. The maximum possible piezometric gradient at the spring, which is the maximum topographic relief divided by the depth to the storage reservoir, is 60%. Therefore, the observed velocity in the hydrothermal system is attainable only if the permeability of the permeable parts of the fault zone is greater than 0.1 darcy.

ACKNOWLEDGEMENTS

This research was supported, in part, through funding provided by U.S.G.S. contract No. 14-08-0001-G-341 and Department of Energy contract No. EG-78-C-07-1601.

REFERENCES

- Blackwell, D.D. and Chapman, D.S., 1977. Interpretation of geothermal gradient and heat flow data for Basin and Range geothermal system. *Geotherm. Resour. Council, Trans.*, 1: 19—20.
- Bodvarsson, G., 1969. On the temperature of water flowing through fractures. *J. Geophys. Res.*, 74: 1987.
- Callaghan, E. and Parker, R., 1961. Geologic map of the Monroe quadrangle, Utah. U.S. Geological Survey.
- Chapman, A.J., 1974. *Heat Transfer*. MacMillan, New York, N.Y.
- Courant, R., Isaacson, E. and Rees, M., 1952. On the solution of non-linear hyperbolic differential equations by finite differences. *Comm. Pure Appl. Math.*, 5: 243.
- Davis, S.N. and DeWiest, R.J.M., 1966. *Hydrogeology*. John Wiley and Sons, New York, N.Y.
- Domenico, P.A. and Palciauskas, V.V., 1973. Theoretical analysis of forced convective heat transfer in regional groundwater flow. *Geol. Soc. Am. Bull.*, 84: 3803—3814.
- Elder, J.C., 1965. Physical processes in geothermal areas. In: W.H.K. Lee (Editor), *Terrestrial Heat Flow*. AGU Monogr., 8: 211—239.
- Gerald, C.F., 1970. *Applied Numerical Analysis*. Addison-Wesley, Reading, Mass.
- Gosman, A.D., Pun, W.M., Runehal, A.K., Spaulding, D.B. and Wolfstein, M., 1969. *Heat and Mass Transfer in Recirculating Flows*. Academic Press, London-New York, N.Y.
- Hahl, D.C. and Mundorff, J.C., 1968. An appraisal of the quality of surface water in the Sevier Lake Basin, Utah, 1964. State Utah Dep. Nat. Resour., Tech. Publ., 19.
- Halliday, M.E., 1978. Gravity and ground-magnetic surveys in the Monroe and Joseph known geothermal resource areas and surrounding region, south-central Utah. M.Sc. Thesis, University of Utah, Logan, Utah.
- Hardy, C.T., 1952. Eastern Sevier Valley, Sevier and Sanpete Counties, Utah. *Utah Geol. Mineral. Surv. Bull.*, 43.

- Hubbert, M.K., 1940. The theory of groundwater motion. *J. Geol.*, 48: 785-944.
- Jaeger, J., 1965. Application of the theory of heat conduction to geothermal measurements. In: W.H.K. Lee (Editor), *Continental Heat Flow. AGU Monogr.*, 8: 7-22.
- Jaffrennou, J.Y., Bories, S.A. and Combournous, M.A., 1974. Convective flows and mean heat transfer in a sloping porous layer. *Proc. 5th Int. Heat Transfer Conf.*, Vol. V, CT 3.5: 83-87.
- Kappelmeyer, D. and Haenel, R., 1974. *Geothermics with Special Reference to Applications.* Geopublication Associates, Gebrüder Borntraeger, Berlin-Stuttgart.
- Keller, G.V. and Frischnecht, F.C., 1966. *Electrical Methods in Geophysical Prospecting.* Pergamon Press, Oxford.
- Lachenbruch, A.H., Sorey, M.L., Lewis, R.E. and Sass, J.H., 1976. The near-surface hydrothermal regime of Long Valley Caldera. *J. Geophys. Res.*, 81: 763-768.
- Le Mehaute, B., 1976. *An Introduction to Hydrodynamics and Water Waves.* Springer-Verlag, New York, N.Y.
- Lowell, R.P., 1975. Circulation in fractures, hot springs, and convective heat transport on mid-ocean ridge crests. *Geophys. J.R. Astron. Soc.*, 40: 351-365.
- Luikov, A.V., 1966. *Heat and Mass Transfer in Capillary-Porous Bodies.* Translated from the Russian version by P.W.B. Harrison. Pergamon Press, Oxford.
- Mase, C.W., 1978. Geophysical survey of the Monroe-Red Hill geothermal system. M.Sc. Thesis, University of Utah, Logan, Utah.
- Miller, C.D., 1976. Alteration and geochemistry of the Monroe known geothermal resource area. M.Sc. Thesis, University of Utah, Logan, Utah.
- Parry, W.T., Benson, N.L. and Miller, C.D., 1976. *Geochemistry and hydrothermal alteration at selected Utah hot springs.* National Science Foundation Contract Report, University of Utah.
- Rosenberger, F.E., 1978. *Fundamentals of Crystal Growth, 1. Macroscopic Equilibrium and Transport Concepts.* Springer-Verlag, Berlin (in press).
- Simon, A.L., 1960. Production analysis of artesian wells. *AWWA*, 52(11): 1444.
- Singh, B.S. and Dybbs, A., 1974. Heat transfer characteristics of porous media. *Proc. 5th Int. Heat Transfer Conf.*, Vol. V, CT3.5: 98-102.
- Slattery, J.C., 1972. *Momentum, Energy, and Mass Transfer in Continua.* McGraw-Hill, New York, N.Y.
- Smith, J.H., 1970. Geothermal development in New Zealand. *Proc. U.N. Symp. on the Development and Utilization of Geothermal Resources, Pisa*, 2: 232-247.
- Sorey, M.L., 1975. Numerical modeling of liquid geothermal systems. *U.S. Geol. Surv. Open-File Rep.*, 75-613.
- Sorey, M.L. and Lewis, R.E., 1976. Convective heat flow from hot springs in the Long Valley Caldera, Mono County, California. *J. Geophys. Res.*, 81: 785-791.
- Stallman, R.W., 1963. Computation of groundwater velocity from temperature data. *U.S. Geol. Surv. Water Supply Paper*, 1544-H: 36-46.
- Stokes, W.L. and Hintze, L.F., 1963. *Geologic map of Utah, southwest quarter.*
- Wilson, W.R. and Chapman, D.S., 1978. Interpretation of heat-flow results at Roosevelt hot springs, Utah. *EOS, Trans. Am. Geophys. Union*, 59(12): 1201.
- Young, R.A. and Carpenter, C.H., 1965. Groundwater conditions and storage in the central Sevier Valley, Utah. *U.S. Geol. Surv. Water Supply Paper*, 1787.

AREA
UT
Sevier
Monroe
Richtin

REFERENCE LIST

Monroe Hot Springs Area and Vicinity, Sevier County, Utah

- MARLETT Anderson, J. J., Rowley, P. D., Fleck, R. J., and Nairn, A., 1975, Cenozoic geology of southwestern high plateaus of Utah: Geol. Soc. America Spec. Paper 160, 88 p.
- ARMSTRONG, R. L., 1968, Sevier orogenic belt in Nevada and Utah: Geol. Soc. American, Bull. v. 79, p. 429-458.
- ESL Brown, R. P., 1974, Regional gravity survey of the Sanpete-Sevier Valleys and adjacent areas in Utah: unpublished M.S. Thesis, Univ. of Utah, 72 p.
- MARLETT Callaghan, E., 1938, Preliminary report on the alunite deposits of the Marysville region, Utah: USGS Bull., no. 886-D.
- ESL Callaghan, E., 1939, Volcanic sequence in the Marysville Region in SW central Utah: Am. Geophys. Union Trans., pt. 3, p. 438-452.
- ESL _____ 1973, Mineral resource potential of Piute County, Utah and adjoining area: Utah Geol. and Mineral Survey, Bull. 102, 135 p.
- ESL _____ 1973, Geological map of the Marysville region, Piute County and parts of adjoining counties, Utah: UGMS Map 34.
- ESL Callaghan, E., and Parker, R. L., 1961a, Geology of Monroe Quadrangle, Utah: U. S. Geol. Survey Map GQ-155.
- ESL Carpenter, C. H., and Young, R. A., 1963, Ground-water data: Central Sevier Valley, parts and Sanpete, Sevier, and Piute Counties, Utah: USGS and Utah Dept. Water Resources, Basic Data Rept. No. 3.
- ESL Caskey, C. F., and Shuey, R. T., 1975, Mid-Tertiary volcanic stratigraphy, Cove Fort area, central Utah: Geology, v. 2, no. 1, p. 17-25.
- ESL Chapman, D. S., and Harrison, Roger, 1978, Monroe, Utah hydrothermal system: Results from drilling of test wells MC1 and MC2: Univ. of Utah, topical report, IDO 76-1601-77-16, 26 p.
- ESL Cook, K. L., and Montgomery, J. R., et al., 1975, Simple Bouguer gravity anomaly map of Utah, UGMS, Map 37.
- Crosby, G. W., 1959, Geology of the South Pavant Range, Millard and Sevier Counties, Utah: Brigham Young Univ., Research Studies, Geology Series, v. 6, no. 3, 59 p.
- ESL _____ 1972, Dual origin of Basin and Range faults, in Plateau-Basin and Range transition zone, central Utah: Utah Geol. Assoc., Publ. no. 2.
- ESL Cunningham, C. G., and Steven, T. A., 1977, Mount Belknap and Red Hills

Calderas and associated rocks, Marysville volcanic field, west-central Utah: U. S. Geol. Survey Open File Report 77-568, 40 p.

- ESL _____ 1978, Geologic map of the Delano Peak NW Quadrangle, west-central Utah: USGS map MF-967.
- ESL EG&G, 1979, Direct heat application, program summary, presented at the Geothermal Resource Council Annual Meeting, Sept. 1979, pp. 41-42.
- ESL Eppich, G. K., 1973, Aeromagnetic survey of south-central Utah: unpublished M.S. Thesis, Univ. of Utah, 78 p.
- ESL Fishman, H. S., 1976, Geologic structure and regional gravity of a portion of the high plateaus of Utah: unpublished M.S. thesis, Univ. of Utah, 134 p.
- ESL Fleck, R. J., Anderson, J. J., and Rowley, P. D., 1975, Chronology of Mid-Tertiary volcanism in high plateaus region in Utah, in *Cenozoic Geol. of SW high plateaus of Utah*: GSA, Spec. Paper 160, p. 53-62.
- ESL Gardner, S., Williams, J. M., and Brougham, G. W., 1976, Audio-Magnetotelluric data log and station location map for Monroe-Joseph KGRA, Utah: U. S. Geol. Survey, Open File Report 76-411.
- ESL Green, S., and Wagstaff, C. W., 1979, Utah Geothermal Commercialization Program: Semi-Annual Report, Jan-June 1979: Utah Division of Water Rights, 49 p.
- ESL Gregory, H. E., 1944, Geologic observations in the upper Sevier River Valley: *Am. Jour. Sci.*, v. 242, p. 277-606.
- ESL Hahl, D. C., and Mundorff, J. C., 1968, An appraisal of the quality of surface water in the Sevier Lake Basin, Utah, 1964: State of Utah Dept. of Natural Res. Tech., Publ. No. 19.
- ESL Halliday, M., and Cook, K. L., 1978, Gravity and ground magnetic surveys in the Monroe and Joseph KGRA's and surrounding region, south-central Utah: Univ. of Utah, Final Report: EY-76-S-07-1601, v. 77-7, 164 p.
- ESL Hanny, J. A., and Lunis, B. C., eds., 1979, Utah hydrothermal commercialization baseline: EG&G-Id. Operations Office.
- ESL Hardy, C. T., 1952, Eastern Sevier Valley, Sevier and Sanpete Counties, Utah: Utah Geol. and Mineralogical Survey, Bull. 43, p. 98.
- ESL Harrison, R. F., 1980, Direct utilization of geothermal resources field experiments at Monroe, Utah: Terra Tek, 7R80-143 Preliminary Draft.
- ESL Heyl, A. V., 1978, Unusual concentrations of elements in Monroe, Utah Hot Springs: Utah Geol. Association, Publication No. 7, p. 71.

- ESL Heylman, E. B., 1966, Geothermal power potential in Utah: UGMS, Spec. Studies No. 14, 29 p.
- ESL Keller, G. R., Smith, R. B., and Braile, L. W., 1975, Crustal structure along the Great Basin-Colorado plateau transition from seismic refraction studies: Jour. Geophys. Res., v. 80, p. 1093-1098.
- ESL Kilty, K., Chapman, D., and Mase, C., 1978, Aspects of forced convective heat transfer in geothermal systems: Univ. of Utah, Topical Report EG-78-C-07-1701, IDO 178-1701.a.6.4.1, 62 p.
- ESL Mackin, J. H., 1960a, Structural significance of Tertiary volcanic rocks in southwestern Utah: Am. Jour. Sci., v. 244, p. 324-356.
- ESL Mariner, R. H., Presser, T. S., and Evans, W. C., 1977, Chemical isotopic, and gas compositions of selected thermal springs in Arizona, New Mexico and Utah: U. S. Geol. Survey, Open File Report 77-654, 42 p.
- ESL Mase, C. W., Chapman, D. S., and Ward, S. H., 1978, Geophysical study of the Monroe-Red Hill geothermal system: Univ. of Utah Technical Report DOE/DGE, Contract 78-C-07-1701.
- ESL Miller, C. D., 1976, Alteration and geochemistry of the Monroe KGRA: Dept. of Geol. and Geophys., M.Sc. Thesis, Univ. of Utah.
- ESL Monroe City, Utah - Municipality, 1977, Proposal for direct utilization of geothermal resources field experiments at Monroe, Utah: Monroe City, P.O. Box A, Monroe, Utah, 84754.
- ESL Mundorff, J. C., 1970, Major thermal springs of Utah: Utah Geol. and Mineral Survey Water Resources, Bull. 13.
- ESL Parry, W. T., Benson, N. L., and Miller, C. D., 1976, Geochemistry and Hydrothermal alteration at selected Utah Hot Springs: Univ. of Utah, Final Report, NSF Grant GI-43741, v. 3, 131 p.
- ESL Ritzma, H. R., 1972, Six Utah "Hingeline" wells in Plateau-Basin and Range Transition Zone, central Utah: Utah Geol. Association, Publ. 2, p. 75-80.
- ESL Rowley, P. D., 1968, Geology of the southern Sevier Plateau, Utah: Ph.D. Dissertation, Univ. of Texas, 327 p.
- ESL Rowley, P. D., Anderson, J. J., and Williams, P. L., 1975, A summary of Tertiary volcanic stratigraphy of the southwestern high plateaus and basin and range provinces in southwestern Utah: Geology, v. 6, p. 51-55.
- ESL Shuey, R. T., Schellinger, D. K., Johnson, E. H., and Alley, L. B., 1973, Aeromagnetics and the transition between the Colorado Plateau and the Basin and Range Province: Geology, v. 1, p. 107-112.

ESL Sontag, R. J., 1965, Regional gravity survey of parts of Beaver, Millard, Piute, and Sevier Counties, Utah: unpublished M.S. Thesis, Univ. of Utah, 32 p.

ESL Sorey, M. L., 1975, Numerical modeling of liquid geothermal systems: USGS, Prof. Paper 1044-D.

ESL Spieker, M., 1946, Late Mesozoic and Early Cretaceous history of central Utah: USGS, Prof. Paper 205-D, p. 117-161.

ESL _____ 1949, The transition between the Colorado Plateaus and the Great Basin in central Utah: Utah Geol. Society, Guidebook No. 4, 106 p.

ESL Steven, T. A., 1978, Geologic map of the Sevier SW Quadrangle, west-central Utah: USGS Map MF-962.

ESL _____ 1979, Geologic map of the Sevier SE Quadrangle, west-central Utah: USGS map MF-1109.

ESL _____ 1979, Geologic map of the Monroe NW Quadrangle, west-central Utah: USGS Field Geol. Map, MF-1107.

ESL _____ 1979, Geologic map of volcanic rocks in the Sevier NE Quadrangle, west-central Utah: USGS MF-1108.

ESL Steven, T. A., Rowley, P. D., and Cunningham, C. G., 1978, Geology of the Marysvale volcanic field, west-central Utah: Brigham Young University Geology Studies, v. 25, part 1, p. 67-70.

ESL Steven, T. A., Rowley, P. D., Hintze, L. F., Best, M. G., Nelson, M. G., Cunningham, C. G., 1978, Preliminary geologic map of the Richfield 10 x 20 Quadrangle, Utah: USGS, OF 78-602.

ESL Steven, T. A., Cunningham, C. G., Naeser, C. W., and Mehnert, H. H., 1977, Revised stratigraphy and radiometric ages of volcanic rocks and mineral deposits in the Marysvale area, west-central Utah: U. S. Geol. Survey Open File Report 77-569, 45 p.

ESL U.S.G.S., 1979, Aeromagnetic map of the Richfield area, Utah: USGS, Open File Report 79-1397.

ESL Young, Richard, A., and Carpenter, Carl H., 1965, Ground-water conditions and storage in the central Sevier valley, Utah: U. S. Geol. Survey Water-Supply Paper, No. 1787.

ESL Zeitz, I., Shuey, R. T., and Kirby, J. R., Jr., 1976, Aeromagnetic map of Utah: USGS, Map GP-907.

REFERENCE LIST

Monroe Hot Springs Area and Vicinity, Sevier County, Utah

- Anderson, J.J., Rowley, P.D., Fleck, R.J., Nairn, A., 1975, Cenozoic Geology of Southwestern High Plateaus of Utah: Geol. Soc. America Spec. Paper 160, 88p.
- Armstrong, R.L., 1968, Sevier Orogenic Belt in Nevada and Utah: Geol. Soc. America, Bull. v. 79, p. 429-458.
- Brown, R.B., 1974, Regional Gravity Survey of the Sanpete-Sevier Valleys and Adjacent Areas in Utah: Unpublished M.S. Thesis, Univ. of Utah, 72p.
- Callaghan, E., 1938, Preliminary Report on the Alunite Deposits of the Marysvale Region, Utah: USGS Bull, no. 886-D.
- Callaghan, E., 1939, Volcanic Sequence in the Marysvale Region in SW Central Utah: Am. Geophys. Union Trans., pt. 3, p. 438-452.
- _____, 1973, Mineral Resource Potential of Piute County, Utah and Adjoining Area: Utah Geol. and Mineral Survey, Bull. 102, 135p.
- _____, 1973, Geol. Map of the Marysvale Region, Piute County and Parts of Adjoining Counties, Utah: UGMS Map 34.
- Callaghan, E., Parker, R.L., 1961a, Geol. of the Monroe Quadrangle, Utah: U.S. Geol. Survey Map GQ-155.
- Carpenter, C.H., Young R.A., 1963, Ground-water Data: Central Sevier Valley, Parts and Sanpete, Sevier, and Piute Counties, Utah: USGS and Utah Dept. Water Resources, Basic Data Report No. 3.
- Caskey, C.F., and Shuey, R.T., 1975, Mid-Tertiary Volcanic Stratigraphy, Cover Fort Area, Central Utah: Geology, v. 2, no. 1, p. 17-25.
- Chapman, D.S., Harrison, Roger, 1978, Monroe, Utah Hydrothermal System: Results from Drilling of Test Wells MCI and MC2: University of Utah, Topical Report, IDO 76-1601-77-16, 26p.
- Cook, K.L., Montgomery, J.R., et.al., 1975, Simple Bouguer Gravity Anomaly Map of Utah, UGMS, Map 37.
- Crosby, G.W., 1959, Geology of the South Pavant Range, Millard and Sevier Counties, Utah: Brigham Young University, Research Studies, Geology Series, v. 6, no. 3, 59p.
- _____, 1972, Dual Origin of Basin & Range Faults, in Plateau-Basin and Range Transition Zone, Central Utah: Utah Geol. Assoc., Publ. no. 2.
- Cunningham, C.G., Steven, T.A., 1977, Mount Belknap and Red Hills Calderas and Associated Rocks, Marysvale Volcanic Field, West-Central Utah: U.S. Geol. Survey Open File Report 77-568, 40p.
- _____, 1978, Geologic Map of the Delano Peak NW Quadrangle, West-Central Utah: USGS Map MF-967.

- EG&G, 1979, Direct Heat Application, Program Summary, Presented at the Geothermal Resource Council Annual Meeting, Sept. 1979, pp. 41-42.
- Eppich, G.K., 1973, Aeromagnetic Survey of South-Central Utah: Unpublished M.S. Thesis, University of Utah, 78p.
- Fishman, H.S., 1976, Geologic Structure and Regional Gravity of a Portion of the High Plateaus of Utah: Unpublished M.S. Thesis, University of Utah, 134p.
- Fleck, R.J., Anderson, J.J., Rowley, P.D., 1975, Chronology of Mid-Tertiary Volcanism in High Plateaus Region in Utah, in *Cenozoic Geol. of SW High Plateaus of Utah*: GSA, Spec. Paper 160, p. 53-62.
- Gardner, S., Williams, J.M., and Brougham, G.W., 1976, Audio-Magnetotelluric Data Log and Station Location Map for Monroe-Joseph KGRA, Utah: U.S. Geol. Survey, Open File Report 76-411.
- Green, S., Wagstaff, C.W., 1979, Utah Geothermal Commercialization Program; Semi-Annual Report, Jan-June 1979: Utah Division of Water Rights, 49p.
- Gregory, H.E., 1944, Geologic Observations in the Upper Sevier River Valley: *Am. Jour. Sci.*, v. 242, p. 277-606.
- Hahl, D.C., Mundorff, J.C., 1968, An Appraisal of the Quality of Surface Water in the Sevier Lake Basin, Utah, 1964: State of Utah Dept of Natural Res. Tech., Publ. No. 19.
- Halliday, Mark, Cook, Kenneth L., 1978, Gravity and Ground Magnetic Surveys in the Monroe and Joseph KGRA's and Surrounding Region, South-Central, Utah: University of Utah, Final Report: EY-76-S-07-1601, v. 77-7, 164p.
- Hanny J.A., Lunis, B.C., eds., 1979, Utah Hydrothermal Commercialization Baseline: EG&G-Id. Operations Office.
- Hardy, C.T., 1952, Eastern Sevier Valley, Sevier and Sanpete Counties, Utah: Utah Geological and Mineralogical Survey, Bull. 43, p. 98.
- Harrison, R.F., 1980, Direct Utilization of Geothermal Resources Field Experiments at Monroe, Utah: Terra Tek, 7R80-143 Preliminary Draft.
- Heyl, A.V., 1978, Unusual Concentrations of Elements in Monroe, Utah Hot Springs: Utah Geol. Association, Publication No. 7, p. 71.
- Heylman, E.B., 1966, Geothermal Power Potential in Utah: UGMS, Spec. Studies No. 14, 29p.
- Keller, G.R., Smith, R.B., Braile, L.W., 1975, Crustal Structure Along the Great Basin-Colorado Plateau Transition from Seismic Refraction Studies: *Jour. Geophys. Res.*, v. 80, p. 1093-1098.
- Kilty, K., Chapman, D., Mase, C., 1978, Aspects of Forced Convective Heat Transfer in Geothermal Systems: University of Utah, Topical Report EG-78-C-07-1701, IDO 178-1701.a.6.4.1, 62p.

- Mackin, J.H., 1960a, Structural Significance of Tertiary Volcanic Rocks in Southwestern Utah: Am. Jour. Sci., v. 244, p. 324-356.
- Mariner, R.H., Presser, T.S., Evans, W.C., 1977, Chemical, Isotopic, and Gas Compositions of Selected Thermal Springs in Arizona, New Mexico and Utah: U.S. Geol. Survey, Open File Report 77-654, 42p.
- Mase, C.W., Chapman, D.S., and Ward, S.H., 1978, Geophysical Study of the Monroe-Red Hill Geothermal System: University of Utah Technical Report DOE/DGE, Contract 78-C-07-1701.
- Miller, C.D., 1976, Alteration and Geochemistry of the Monroe KGRA: Dept. of Geol. and Geophys., M.Sc. Thesis, University of Utah.
- Monroe City, Utah - Municipality, 1977, Proposal for Direct Utilization of Geothermal Resources Field Experiments at Monroe, Utah: Monroe City, P.O. Box A, Monroe, Utah 84754.
- Mundorff, J.C., 1970, Major Thermal Springs of Utah: Utah Geol. and Mineral Survey Water Resources, Bull. 13.
- Parry, W.T., Benson, N.L., and Miller, C.D., 1976, Geochemistry and Hydrothermal Alteration at Selected Utah Hot Springs: University of Utah, Final Report, NSF Grant GI-43741, v. 3, 131p.
- Ritzma, H.R., 1972, Six Utah "Hingeline" Wells in Plateau-Basin and Range Transition Zone, Central Utah: Utah Geol. Association, Publ. 2, p. 75-80.
- Rowley, P.D., 1968, Geology of the Southern Sevier Plateau, Utah: Ph.D. Dissertation, University of Texas, 327p.
- Rowley, P.D., Anderson, J.J., and Williams, P.L., 1975, A Summary of Tertiary Volcanic Stratigraphy of the Southwestern High Plateaus and Adjacent Great Basin, Utah: U.S. Geol. Survey Bull. 1405-B.
- Rowley, P.D., Anderson, J.J., William, P.L, and Fleck, R.L., 1978, Age of Structural Differentiation Between the Colorado Plateaus and Basin and Range Provinces in Southwestern Utah: Geology, v. 6, p. 51-55.
- Shuey, R.T., Schellinger, D.K., Johnson, E.H., and Alley, L.B., 1973, Aeromagnetics and the Transition Between the Colorado Plateau and the Basin and Range Province: Geology, v. 1, p. 107-112.
- Sontag, R.J., 1965, Regional Gravity Survey of Parts of Beaver, Millard, Piute, and Sevier Counties, Utah: Unpublished M.S. Thesis, University of Utah, 32p.
- Sorey, M.L., 1975, Numerical Modeling of Liquid Geothermal Systems: USGS, Prof. Paper 1044-D.
- Spieker E.M., 1946, Late Mesozoic and Early Cretaceous History of Central Utah: USGS, Prof. Paper 205-D, p. 117-161.
- _____, 1949, The Transition Between the Colorado Plateaus and the Great Basin in Central Utah: Utah Geol. Society, Guidebook No. 4, 106p.

Steven, T.A., 1978, Geol. Map of the Sevier SW Quadrangle, West-Central Utah: USGS Map MF-962.

____ 1979, Geol. Map of the Sevier SE Quadrangle, West-Central Utah: USGS Map MF 1109.

____ 1979, Geol. Map of the Monroe NW Quadrangle, West-Central Utah: USGS, Field Geol. Map, MF-1107.

____ 1979, Geol. Map of Volcanic Rocks in the Sevier NE Quadrangle, West-Central Utah: USGS MF-1108.

Steven, T.A., Rowley, P.D., Cunningham, C.G., 1978, Geology of the Marysvale Volcanic Field, West-Central Utah: Brigham Young University Geology Studies, v. 25, part 1, p. 67-70.

Steven, T.A., Rowley, P.D., Hintze, L.F., Best, M.G., Nelson, M.G., Cunningham, C.G., 1978, Preliminary Geol. Map of the Richfield 1°x2° Quadrangle, Utah: USGS, OF 78-602.

Steven, T.A., Cunningham, C.G., Naeser, C.W., and Mehnert, H.H., 1977, Revised Stratigraphy and Radiometric Ages of Volcanic Rocks and Mineral Deposits in the Marysvale Area, West-Central Utah: U.S. Geol. Survey Open File Report 77-569, 45p.

U.S.G.S., 1979, Aeromagnetic Map of the Richfield Area, Utah: USGS, Open File Report 79-1397.

Young, Richard, A., and Carpenter, Carl H., 1965, Ground-Water Conditions and Storage in the Central Sevier Valley, Utah: U.S. Geol. Survey Water-Supply Paper, No. 1787.

Zeit, I., Shuey, R.T., Kirby, J.R., Jr., 1976, Aeromagnetic Map of Utah: USGS, Map GP-907.

UNIVERSITY OF UTAH RESEARCH INSTITUTE

UURI

EARTH SCIENCE LABORATORY
420 CHIPETA WAY, SUITE 120
SALT LAKE CITY, UTAH 84108
TELEPHONE 801-581-5283

August 6, 1979

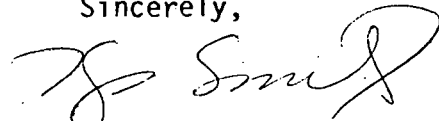
Roger Harrison
Terra Tek
420 Wakara Way
Salt Lake City, UT 84108

Dear Roger:

On July 17, 1979 you requested a brief analysis of pump-test data from an artesian geothermal well at Monroe, Utah. Curve-fitting techniques were used to quantify the hydrologic properties of the alluvial aquifer and to estimate the distance to an infinite-recharge boundary, the Sevier fault. More elaborate testing and modeling will be required to evaluate the hydrologic properties of the fault.

This analysis of the 70-hour pump-test indicates that the 1471 foot deep well can be outfitted to produce as much as 600 gpm (gallons per minute), enough to satisfy the projected near-term requirements for the City of Monroe. Additional development of the well and a larger pump will be required to meet this peak demand. It is doubtful that the alluvium at the Monroe "Mound" can support greater discharges. Any future production wells should be sited near Red Hill.

Sincerely,



Kip Smith
Associate Geophysicist

KS:ls

Encl.

MONROE KGRA PUMP TEST ANALYSIS

by

Christian Smith

The flowing geothermal well at Monroe, Utah was pumped at a reported average rate of 330 gpm for 70 hours. This report summarizes the data, their utility, and the results of this successful pump-test. The results favor the limited development of the hydrothermal system and can be better appreciated in the light of the geologic and geophysical background material provided by Mase et al (1978).

Figure 1 is a sketch of the pumped well and the geologic units it penetrates. The 9 5/8 inch hole enters a 400 foot thick limestone, playa or limestone conglomerate below the valley fill. This unit is consolidated and may impede the vertical migration of thermal fluids. The well penetrates the Sevier fault system that acts as the conduit for upwelling thermal fluids at a depth near 1100 feet. The hole bottomed at 1471 feet, is open below 1313 feet and was completed with 7 5/8 inch slotted casing in the interval between 945 and 1313 feet. The well is cased off from all formations above 945 feet.

This construction seriously constrains the performance of the well and the response of the two observation wells that are completed in the alluvium. The lime-rich unit separates the producing interval of the pumped well (945-1471 feet) from the alluvium tapped by the monitor wells. Estimates of transmissivity from the production well and the deeper monitor well (MC-2) can be expected to be lower than those from the shallower monitor well (MC-1). The alluvium above the lime-rich unit may communicate only partially with the deeper producing interval especially at early times in the pump test.

A more serious complication is the presence of the Sevier fault system. The hot springs at Monroe and Red Hill occur at apparent changes in the trend of the surface trace of the Sevier fault. Several heat-flow holes located near the fault trace are isothermal (Mase et al 1978). An interpretation of precision gravity data indicates a calculated throw of 1760 meters (5800 feet) along three parallel step faults within the fault system. This throw may be sufficient to juxtapose a permeable massive granular aquifer (Jurassic Navajo Sandstone) against tight welded tuffs (Tertiary Bullion Canyon Volcanics). Mase et al (1978) suggest that the Navajo Sandstone yields thermal fluids to the fault system at depth and that surface discharge is controlled by flexures in the fault system. Wells that tap the fault system or adjacent permeable material respond to the endless quantity of recharge it supplies. They respond much like wells drilled in the shore of a large deep lake: they very quickly begin to draw water from the lake and give little information about the material in which they are completed.

The monitor wells do not penetrate the fault system but are in hydraulic communication with it. When the pumped well intercepts water flowing in the fault system it deprives the alluvial aquifer of this water. The response of the monitor wells is indicative of the hydraulic properties of the alluvium, not of the fault. No quantitative assessment of the hydraulic properties of the fault system can be made from the data from this pump test. An additional pump test will be required and is recommended in the concluding remarks.

The results of the pump test analyses are given in Table 1. They are internally consistent and are supported with sufficient data. A brief discussion of each analysis follows some general comments on the reliability of the various types of analyses used.

TABLE 1

SUMMARY OF PUMP TEST RESULTS

WELL	ANALYSIS TYPE	TRANSMISSIVITY	STORAGE	COMMENTS
		FT ² /day	%	
Production	Semilog Drawdown	170	--	Unreliable, Fig. 3
	Semilog recovery	400	--	Unreliable, Fig. 4
MC-1	Stallman drawdown	560	.002	360 ft. deep, Fig. 5
	Stallman recovery	470	.004	400 ft. to fault, Fig. 7
MC-2	Theis drawdown	460	.003	620 ft. deep, Fig. 6
	Stallman recovery	280	.001	600 ft. to fault, Fig. 8
Production	Semilog drawdown	350	--	after stimulation, Fig. 10

Table 1 shows a range of estimated transmissivities from 170 to 560 feet²/day. The low value (170 feet²/day) is unreliable. It is the product of a straight-line, semilogarithmic approximation to the Theis (1935) solution to the equation of transient ground-water flow. The Theis solution assumes that a homogeneous isotropic aquifer with a constant storage coefficient has been fully penetrated by all wells used in the test. When any of these assumptions is invalid, the semilog approximation produces erroneous results. It is, however, the only method that can be used to assess data from a pumping well. The range between the remaining six estimates of transmissivity is small and probably represents the true heterogeneity of the aquifer.

The semilog approximation cannot be used to estimate the storage coefficient. The estimates from the two monitor wells are typical of artesian systems in poorly consolidated materials. Table 1 suggests that the aquifer is more confined at 620 feet than it is at 360 feet.

The values given in Table 1 are representative for the aquifer material that separates the pumped well and the monitor wells. Lithologic logs given by Mase et al (1978) suggest that the aquifer is composed of gravel with minor clay: coarse valley-fill alluvium. The low values of transmissivity suggest a higher percentage of fine material than they indicate. It is realistic to suppose that much of the silt or clay fraction was not observed in drill cuttings. The aquifer responds like a fine-grained, fairly tight, poorly consolidated sediment. The restricted area of low resistivity near the wells (Mase et al 1978) supports the contention that the aquifer is "tight".

Figure 2 is a log-log plot of drawdown in the pumping well as a function of time. Wells that pump compressible fluids display a unit slope at early times. Since no unit slope is seen, Figure 2 indicates that the thermal fluids contain only a small fraction of dissolved gasses. It also reveals that data taken at small times can be used validly to assess transmissivity and storage (Earlougher, 1977).

Figure 3 is a plot of drawdown in the pumping well as a function of the logarithm of time (the semilog plot discussed above). The straight line approximation to the Theis solution yields a low estimate of transmissivity (170 feet²/day). This low value suggests that the well may have been inefficient. (Its efficiency was improved by surging after the test was completed.) The most interesting features of the plot are the halving of the slope and the horizontal line that appears after about half an hour. These features indicate that the well is producing water from a lateral inhomogeneity, an "infinite" recharge boundary--the Sevier fault system conduit. Unfortunately, the uniform drawdown after half an hour precludes any analysis of the transmissivity of the fault system

After 70 hours of pumping, the well was shut in and the recovery of the water level monitored. Figure 4 is the plot of the recovery as a function of the logarithm of the ratio between the time since the pump started (t) to the time since the pump stopped (t'). This ratio of times is always used when plotting recovery data because the recovery is a function of both pumping time and recovery time. When the pump has just been shut off ($t \gg t'$), the ratio is large and plots near the right-hand side of the graph. As recovery progresses, the data points "move" from right to left.

Three straight lines appear on Figure 4. The steepest line appears at the earliest time and represents the interval when interstitial storage is being replenished. The slope of the second line produces an estimate of transmissivity of 700 feet²/day; that of the third line 400 feet²/day, nearly half. This halving again suggests the influence of a recharge boundary. Only the third line can be expected to yield a reliable (?) estimate of transmissivity

Since the fault system affected the drawdown and recovery of the pumped well, an attempt was made to assess its impact on the monitor wells. Figure 5 is a Stallman (1963) analysis of the drawdown in monitor well MC-1. No recharge boundary was noted. The curve follows the Theis solution and yields reliable estimates for both transmissivity and the coefficient of storage. Figure 6 is a conventional Theis curve analysis of the drawdown in monitor well MC-2. It too shows no effect of the recharge boundary and yields reliable estimates.

Figure 1 may help explain why the effect of the fault system is not apparent in the drawdown data from the monitor wells. When the pumped well intercepts the water flowing up the fault system, the water in the alluvial

aquifer responds by reversing its usual direction of flow. The fault system acts as a drain. The rate at which the aquifer drains is dependant only on the hydraulic properties of the alluvium, not on those of the fault system.

On the other hand, when the pump is shut off, water begins to rise along the fault system and to infiltrate the alluvial aquifer. The recovery of the monitor wells is dependant not only on the hydraulic properties of the alluvium but also on their distance to the source of recharge. The nearer a well is to the recharge boundary, the sooner the recharge will effect its recovery. Figures 7 and 8 are Stallman plots of the recoveries in monitor wells MC-1 and MC-2 respectively. MC-1 responds to the recharge much more quickly then MC-2. Well MC-1 is estimated by the Stallman method to be about 400 feet and well MC-2 to be about 600 feet from the fault system. Both analyses give reasonable estimates for transmissivity and storage.

Figure 9 is a sketch map, provided by Terra Tek, of the well locaions. The circles are the radii to the Sevier fault system recharge boundary computed by the Stallman method. If the distances are correct, the intersections of the circles ought to reveal the most probable areas where the fault system is acting as a conduit. In this case the circles intersect northeast of the wells, in the direction of Red Hill. The thermal fluids at Monroe may be flowing from near Red Hill. Future exploratory drilling should be sited closer to Red Hill. A spontaneous potential (SP) survey may delineate the conduit area if cultural noise is sufficiently low.

After the wells had recovered to near their pre-pumping levels, development of the pumped well was undertaken by surging. A short-term (2 hr) drawdown test was then performed to evaluate the success of the development. Figure 10 is a semilog plot of this drawdown. It displays two distinct

straight lines, the slope of the second is half that of the first. The fault system was again encountered. However, the pumping was not continued long enough for the drawdown to become constant, as it did during the 70-hour pump-test. Had the test continued for a day, the drawdown would have stabilized. The estimate of transmissivity (350 feet²/day) agrees well with all the estimates given above and indicates that the surging operation was successful.

The success of the surging operation encourages the following proposal for continued hydrologic field work. The well can probably be improved even more with conventional, commercial techniques (acidizing, etc.). Following the additional development a 12- or 24-hr multiple-rate pump test should be conducted. The first flow rate should be less than 400 gpm and should be held constant until the drawdown level has stabilized for at least half a log cycle. The flow rate should then be instantaneously increased to above 400 gpm and the water level again allowed to stabilize. If time and pumping power allow, this process of step increases in discharge should be repeated. The final flow rate should be about 250 gpm--barely more than the natural artesian flow. The resulting drawdowns in the pumped well and the monitor wells can be analyzed to assess the hydraulic properties of the fault system.

The values given in Table 1 suggest that 450 feet²/day and 0.003 are reasonable averages for the estimates of transmissivity and storage. To determine whether these averages reproduce the observed drawdowns at the end of the pumping period, the Theis solution was calculated for 70 values of distance from the pumped well, Table 2. The agreement is very good at 340 feet from the pumped well, the distance to monitor well MC-1 but not so good at 165 feet, the distance to well MC-2. This may be due to the lower average

transmissivity shown for well MC-2 in Table 1. Granting the documented stratigraphic and structural inhomogeneity of the area, the disagreement is not a cause for alarm.

Tables 3 and 4 show the predicted drawdowns at distances as great as a mile for the Monroe well pumping 600 gpm for periods of 2 and 8 days. These predictions reveal that the well can be pumped "safely" for longer than a week at 600 gpm. The estimated drawdowns do not take into account the "infinite" recharge boundary effect of the Sevier fault system and therefore represent greater-than-expected declines in water level.

CONCLUSIONS

- 1) The Monroe well can safely yield 600 gpm for periods as long as a week.
- 2) The thermal fluids rise along the fault system and communicate with the alluvial aquifer in an area northeast of the wells, in the direction of Red Hill.
- 3) Future exploratory drilling should be sited near Red Hill.
- 4) The Monroe well should be further developed and a step drawdown test (with recovery) be conducted to assess the degree of hydraulic communication between the alluvium and the Sevier fault system.

REFERENCES CITED

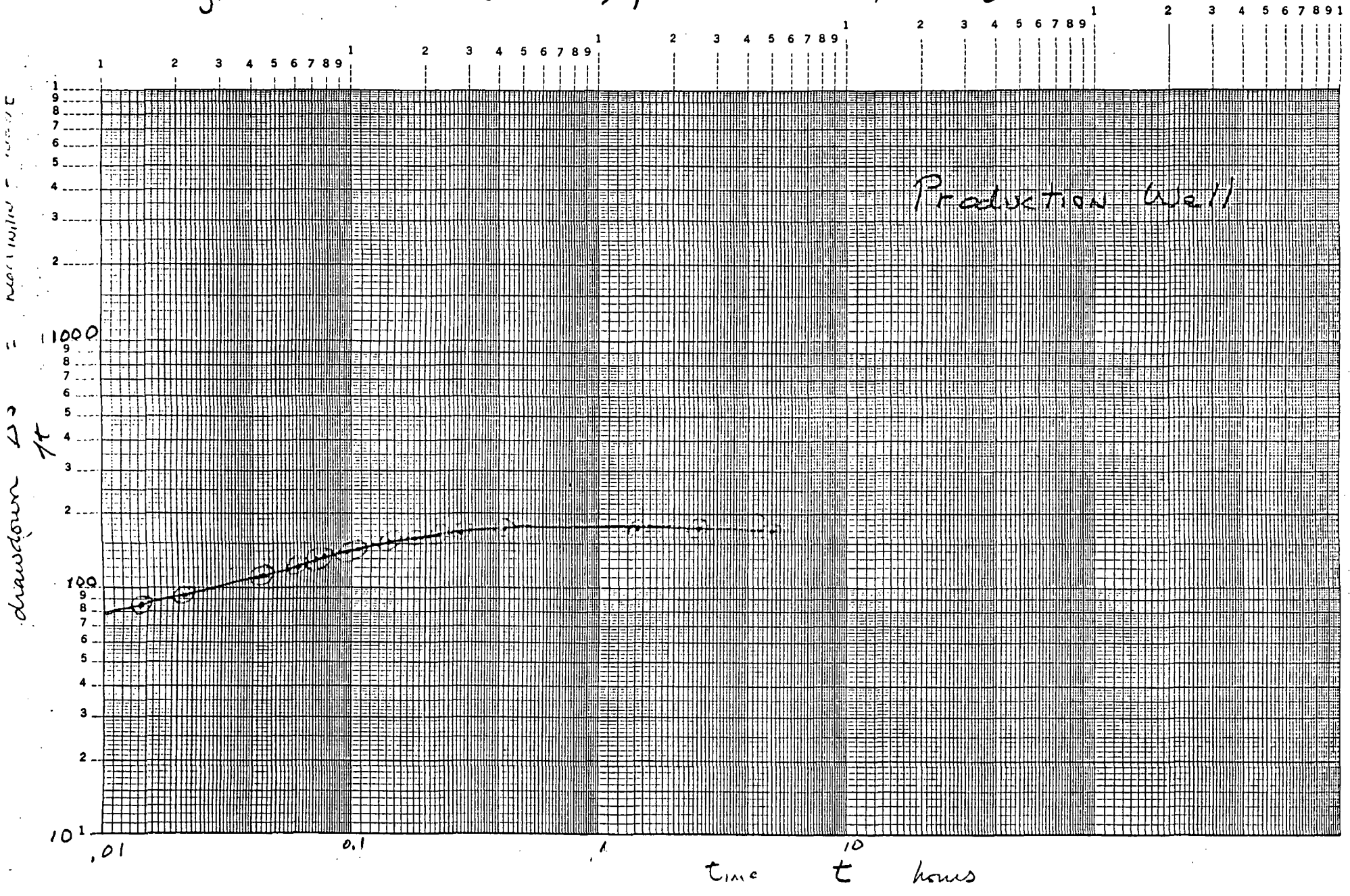
Earlougher, R. C., Jr., 1977, Advances in well test analysis: Monograph 5, Soc. Pet. Eng. AIME, 264 p.

Mase, C. W., Chapman, D. S., and Ward, S. H., 1978, Geophysical study of the Monroe--Red Hill geothermal system: Univ. Utah Dept. Geol. and Geophysics, Topical Report., DOE grant EY-76-S-07-1601, 89 p.

Theis, C. V., 1935, The relation between the lowering of the piezometric surface and the rate and duration of discharge of a well using ground-water storage: Am. Geophys. Union Trans., v. 16, p. 519-524.

Stallman, R. W., 1963, Type curves for the solution of single boundary problems, in Bentall, Ray, compiler, Shortcuts and special problems in aquifer tests: U. S. Geol. Survey Water-Supply Paper 1545-C, p. C45-47.

Fig. 2 Drawdown vs Time, production well, log-log



Test for wellbore storage

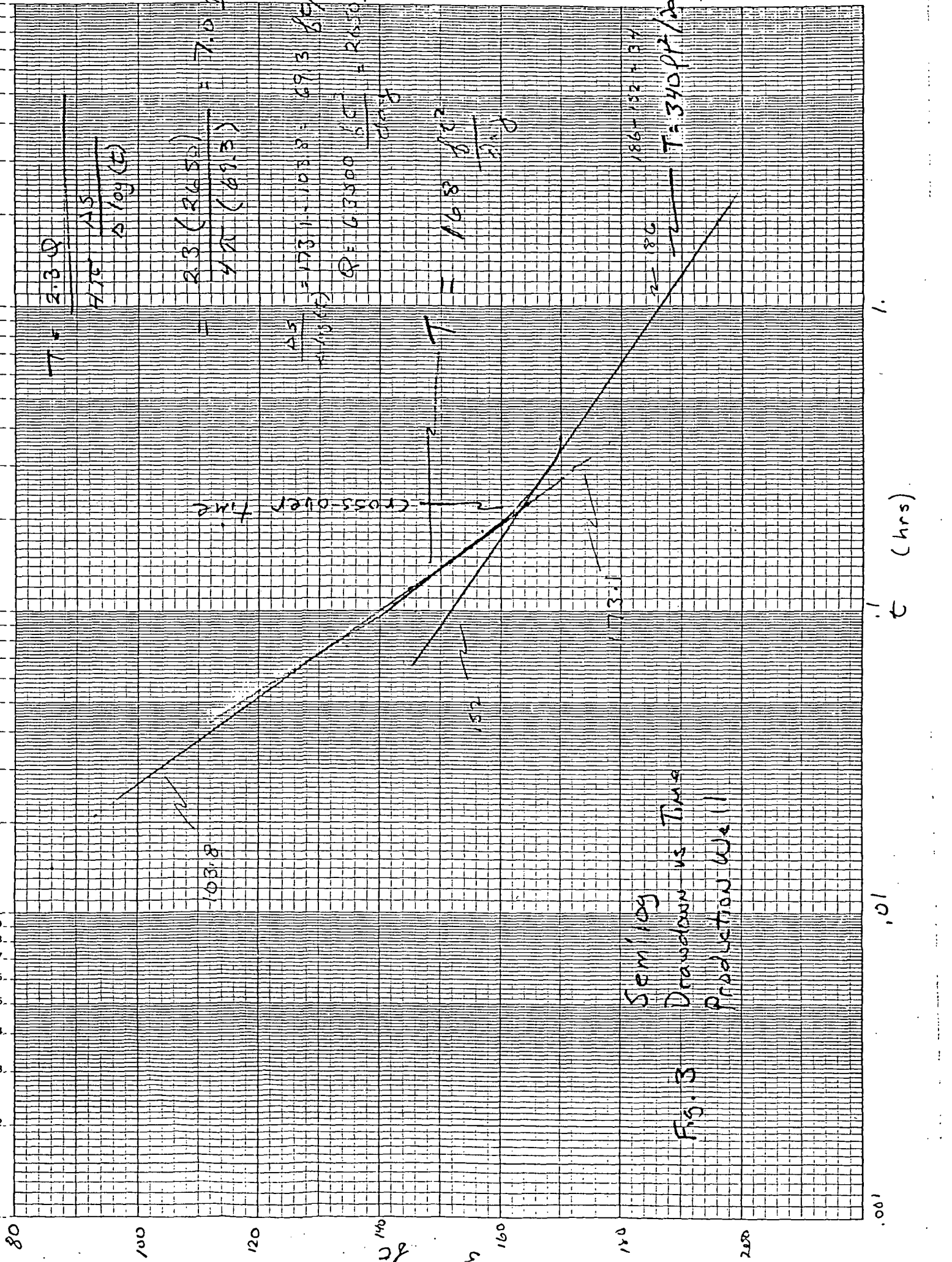


Fig. 3
 Semilog Drawdown vs Time
 Production Well

$$T = 2.30 \frac{AS}{\Delta \log(t)}$$

$$= \frac{2.3 (265)}{4 \log(69.3)} = 7.0 \frac{10^4}{hr}$$

$$\frac{AS}{\Delta \log(t)} = 173.1 - 103.8 = 69.3 \frac{ft}{ms}$$

$$Q = 63000 \frac{bbl}{day} = 2450 \frac{ft^3}{hr}$$

$$= 16.8 \frac{ft^3}{day}$$

$$186.152 = 87$$

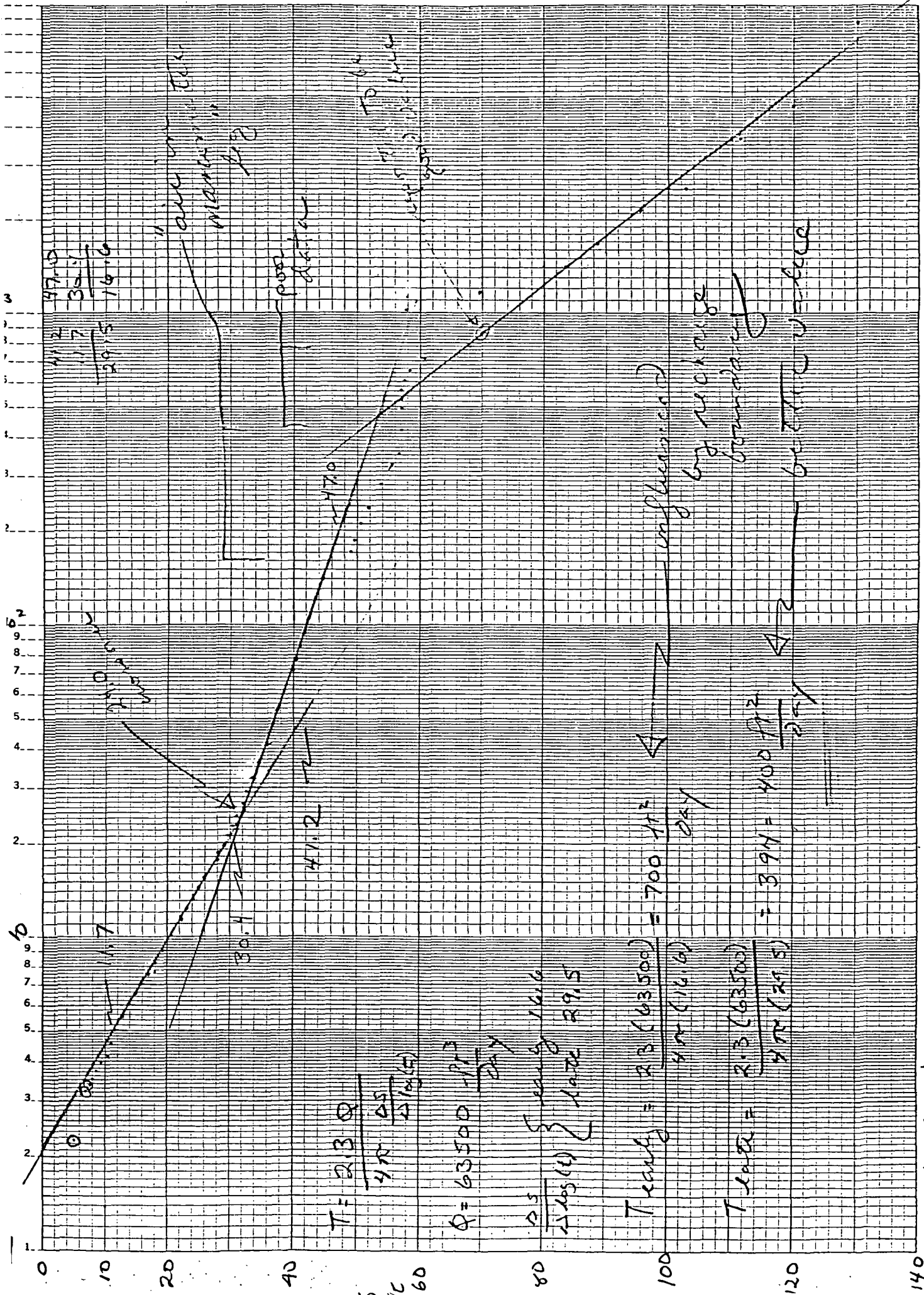
$$T = 340.2 \text{ (hrs)}$$

cross-over time

t (hrs)

101

100



$$\frac{41.2}{11.7} = \frac{63500}{2915}$$

$$\frac{3.5}{16.6} = \frac{63500}{2915}$$

$$T = \frac{213 Q}{4R \frac{AS}{216.6}}$$

$$Q = 63500 \frac{11.7}{2915}$$

$$\frac{AS}{216.6} \left\{ \begin{array}{l} \text{avg } 16.6 \\ \text{rate } 2915 \end{array} \right.$$

$$T_{\text{recovery}} = \frac{213 (63500)}{4R (16.6)} = 700 \frac{11.7}{\text{day}}$$

$$T_{\text{recovery}} = \frac{213 (63500)}{4R (21.5)} = 394 = 400 \frac{11.7}{\text{day}}$$

pool elevation
by technique
boundary effect

63500
2915

Fig 4- Semilog recovery production well

$$t_1 = \frac{t + t'}{T}$$

day t = time since pump on
day t' = time since pump off

Fig 5 Stallman log-log drawdown, Well MC-1 - no sign of recharge boundary

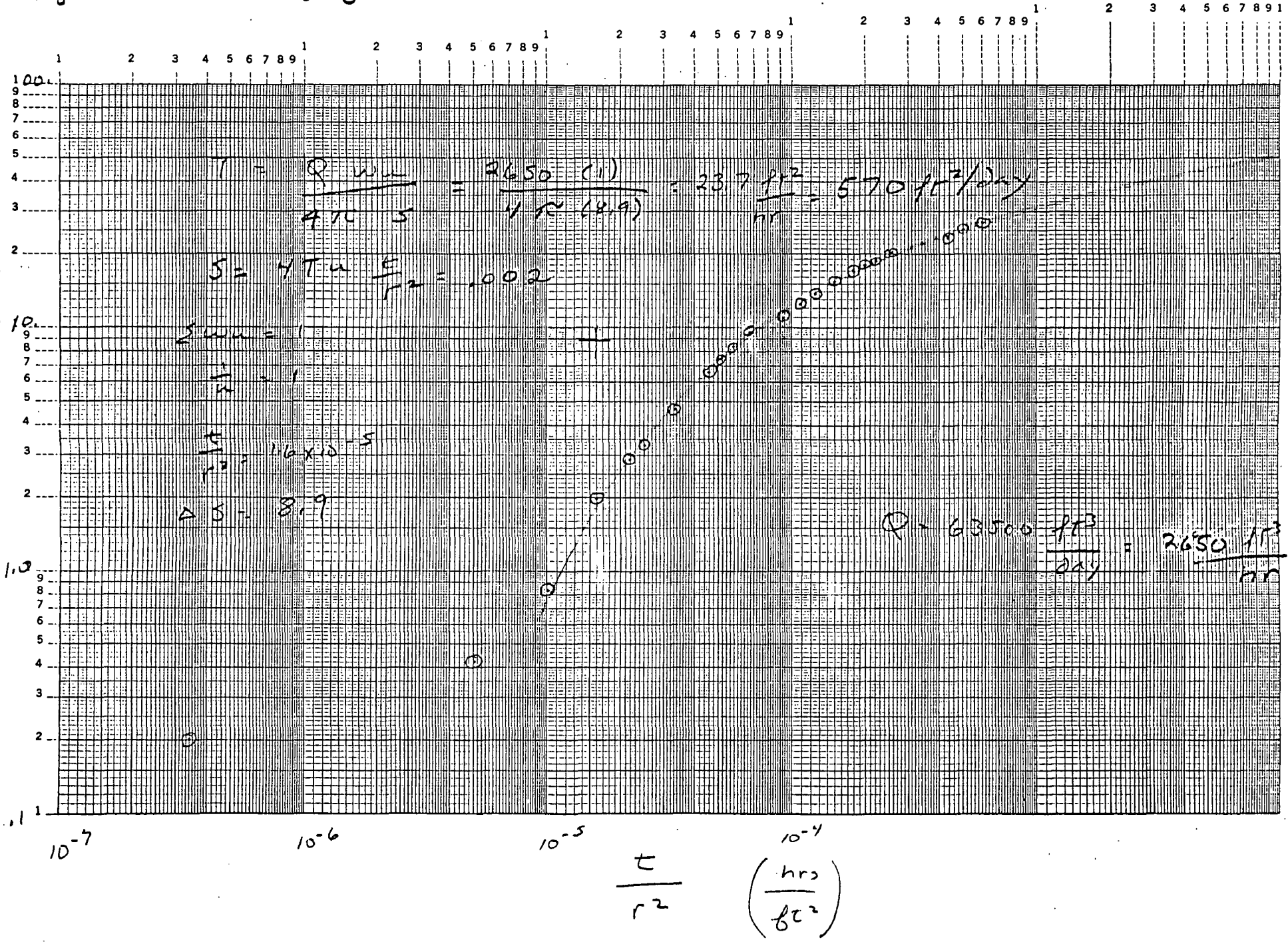
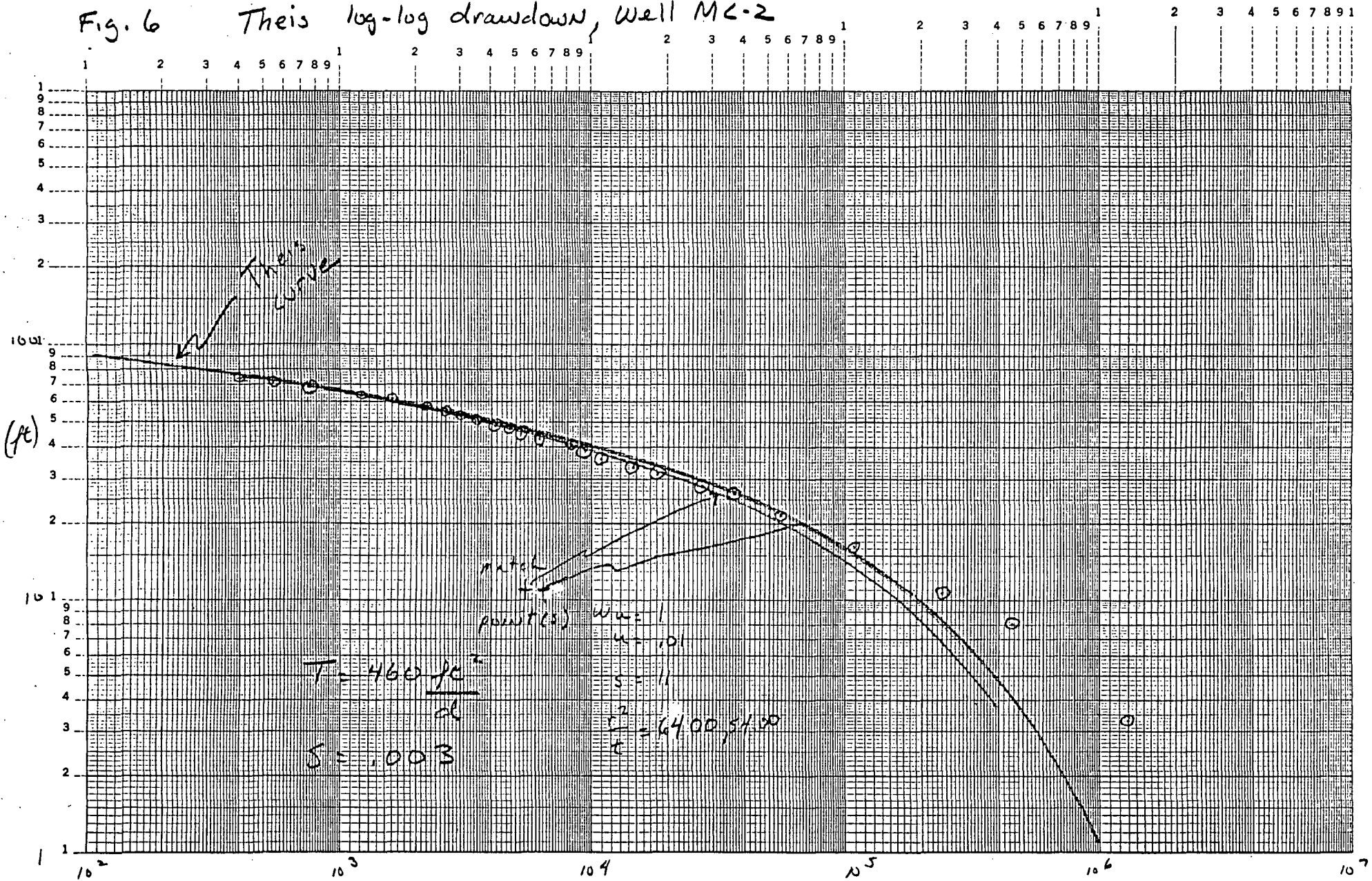


Fig. 6 Theis log-log drawdown, Well MC-2



$$\frac{r^2}{t} \quad \frac{ft^2}{day}$$

Fig. 7 Stallman log-log recovery, well MC-1

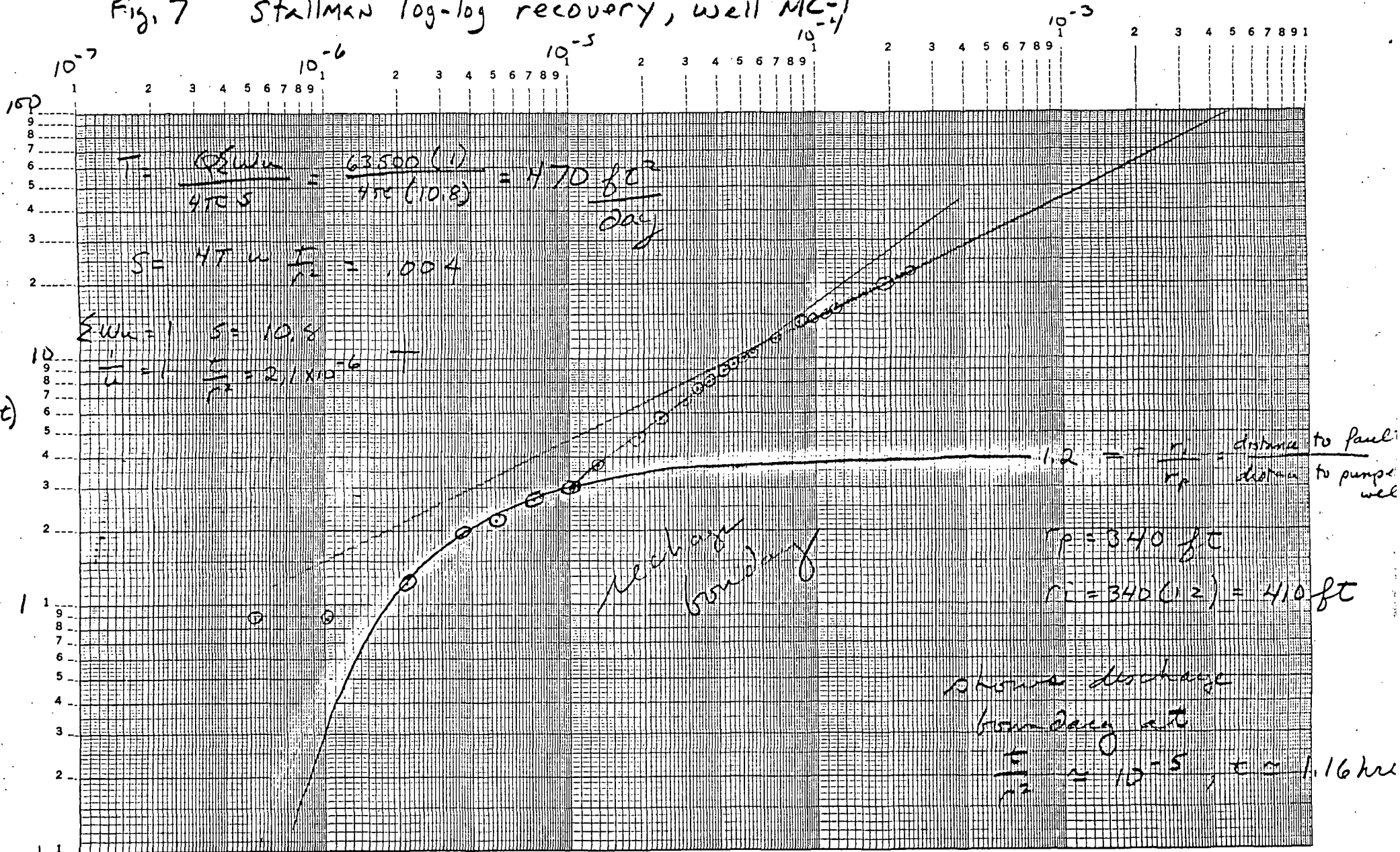
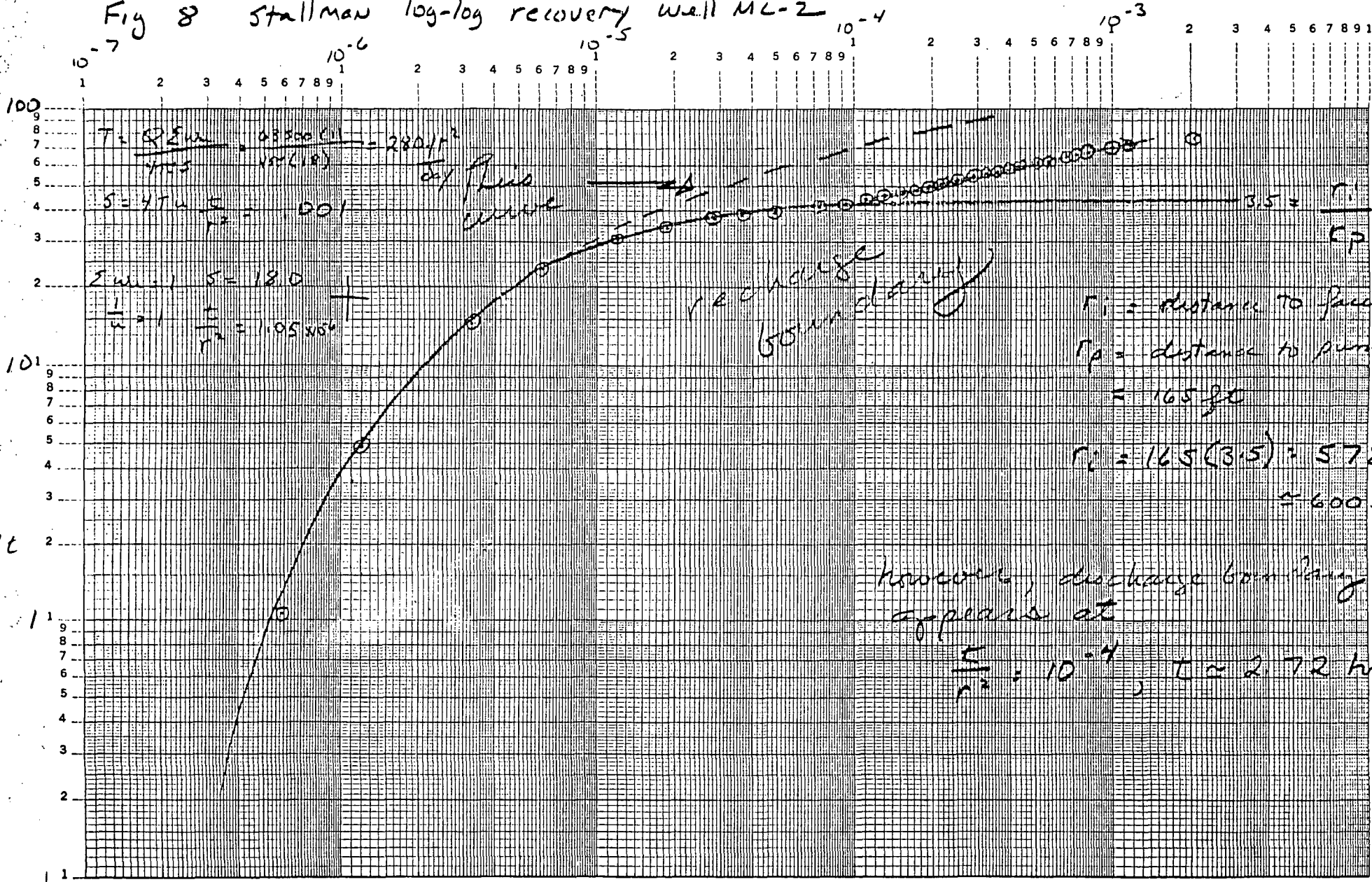


Fig 8 Stallman log-log recovery well MC-2



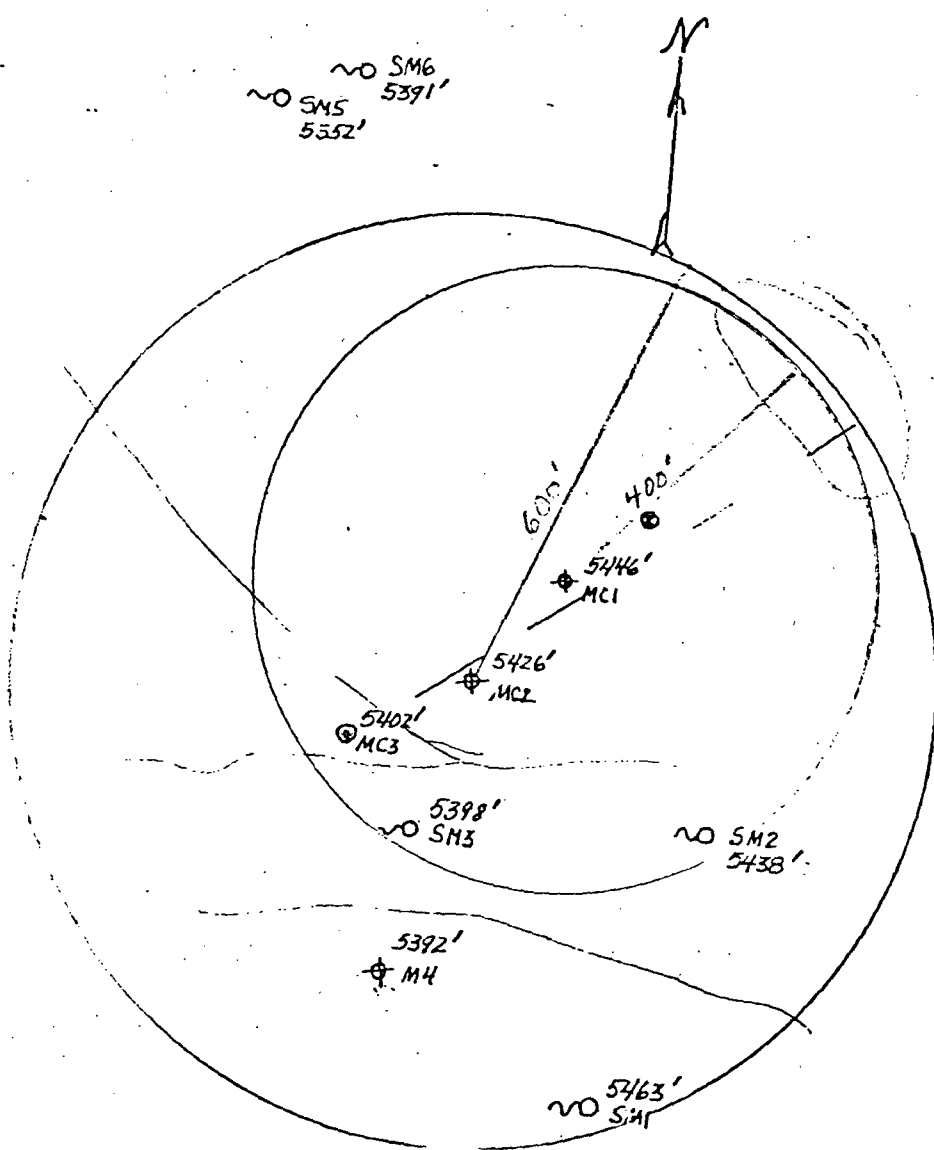
$$\frac{t}{r^2} \left(\frac{\text{hr}}{\text{ft}^2} \right)$$

$r = 165'$

Well Depth

MC1	360'
MC2	620'
MC3	1471'
M4	247'
RH _H	205'

MAP OF SPRINGS AND WELLS AT MONROE MOUND



Red Hill
 ↗
 ↗ RH hot Spring and RH mound, hole
 N 45.6° E
 N 3060'

LEGEND

- no SPRING
- Section Corner
- ⊕ Observation Well
- ⊙ Production Well

Scale 1mm = 10'

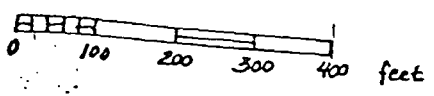


Fig 9 Inferred distances to recharge ()

$$T = \frac{2.13 \times 2}{\frac{1}{19.6} + \frac{1}{39.8}} = 10.96 = 69.8 \text{ ft}$$

$$T_{avg} = \frac{2.13 (76,000)}{470 \times 39.8} = 350 \frac{\text{ft}^2}{\text{day}}$$

$$T_{avg} = \frac{2.13 (72,400)}{470 \times 19.6} = 675 \frac{\text{ft}^2}{\text{day}}$$

$$T_{avg} = \frac{2.13 (76,000)}{470 \times 39.8} = 350 \frac{\text{ft}^2}{\text{day}}$$

$$T_{avg} = \frac{2.13 (72,400)}{470 \times 19.6} = 675 \frac{\text{ft}^2}{\text{day}}$$

$$T_{avg} = \frac{2.13 (76,000)}{470 \times 39.8} = 350 \frac{\text{ft}^2}{\text{day}}$$

$$T_{avg} = \frac{2.13 (72,400)}{470 \times 19.6} = 675 \frac{\text{ft}^2}{\text{day}}$$

$$T_{avg} = \frac{2.13 (76,000)}{470 \times 39.8} = 350 \frac{\text{ft}^2}{\text{day}}$$

$$T_{avg} = \frac{2.13 (72,400)}{470 \times 19.6} = 675 \frac{\text{ft}^2}{\text{day}}$$

$$T_{avg} = \frac{2.13 (76,000)}{470 \times 39.8} = 350 \frac{\text{ft}^2}{\text{day}}$$

$$T_{avg} = \frac{2.13 (72,400)}{470 \times 19.6} = 675 \frac{\text{ft}^2}{\text{day}}$$

$$T_{avg} = \frac{2.13 (76,000)}{470 \times 39.8} = 350 \frac{\text{ft}^2}{\text{day}}$$

$$T_{avg} = \frac{2.13 (72,400)}{470 \times 19.6} = 675 \frac{\text{ft}^2}{\text{day}}$$

$$T_{avg} = \frac{2.13 (76,000)}{470 \times 39.8} = 350 \frac{\text{ft}^2}{\text{day}}$$

$$T_{avg} = \frac{2.13 (72,400)}{470 \times 19.6} = 675 \frac{\text{ft}^2}{\text{day}}$$

$$T_{avg} = \frac{2.13 (76,000)}{470 \times 39.8} = 350 \frac{\text{ft}^2}{\text{day}}$$

$$T_{avg} = \frac{2.13 (72,400)}{470 \times 19.6} = 675 \frac{\text{ft}^2}{\text{day}}$$

doublet well in
infinite discharge
boundary

Fig. 10
Semilog
drawdown
production well
AFTER SURGING

400
380
360

10
26
45
75
97

Q = 400(10) + 384(6.5)
= 395 gpm = 76,000 ft³/day
Q = 384(9.5) + 380(7) + 375(5)
= 370(22)
= 80.5

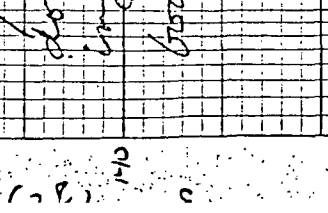
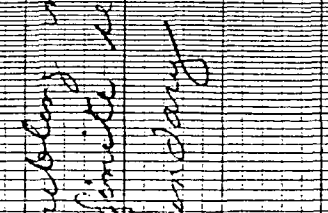
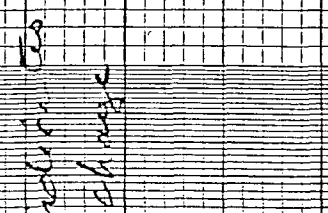
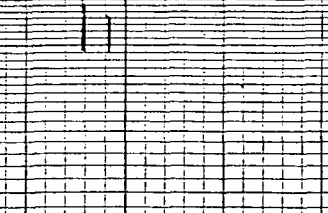
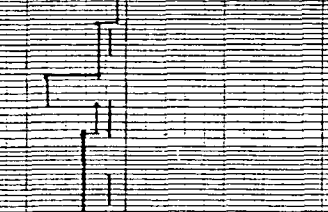
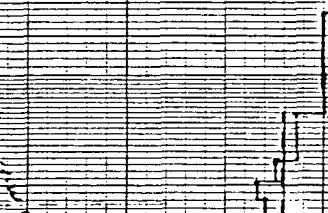
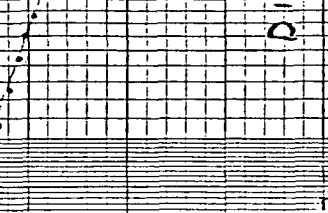
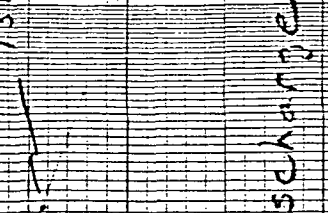
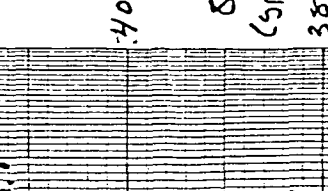
1. = 376 gpm = 72,400 ft³/day

1. = 376 gpm = 72,400 ft³/day

1. = 376 gpm = 72,400 ft³/day

1. = 376 gpm = 72,400 ft³/day

1. = 376 gpm = 72,400 ft³/day



400
380
360

10
26
45
75
97

Q = 400(10) + 384(6.5)
= 395 gpm = 76,000 ft³/day
Q = 384(9.5) + 380(7) + 375(5)
= 370(22)
= 80.5

1. = 376 gpm = 72,400 ft³/day

1. = 376 gpm = 72,400 ft³/day

1. = 376 gpm = 72,400 ft³/day

1. = 376 gpm = 72,400 ft³/day

1. = 376 gpm = 72,400 ft³/day

1. = 376 gpm = 72,400 ft³/day

1. = 376 gpm = 72,400 ft³/day

DRAWDOWN # 1
 T= 450.0000 S= .0030 G= 600.0000 TIME= 2.0000

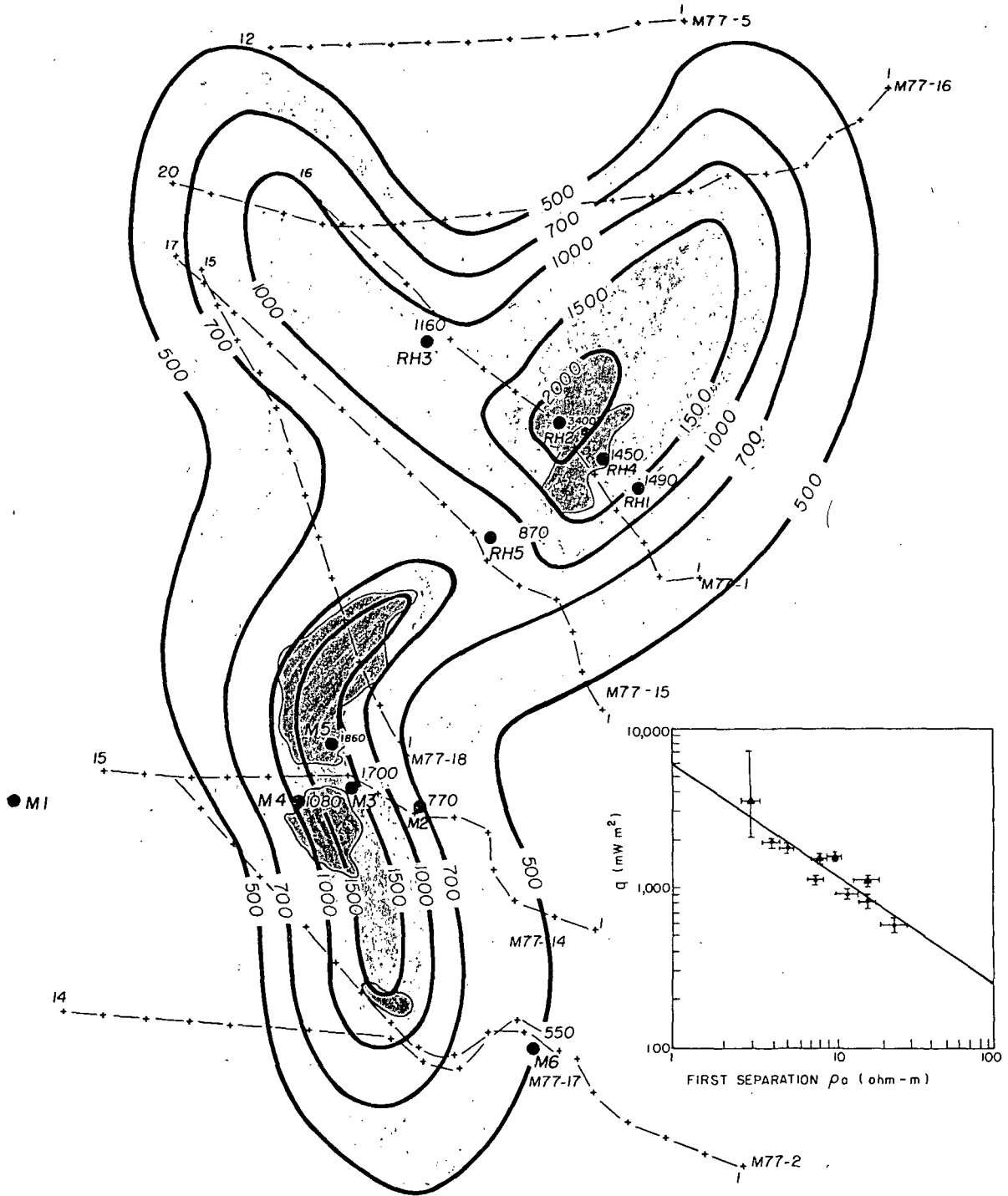
A	DISTANCE	DRAWDOWN			
1	1.0000	274.113			
2	1.2000	266.666			
3	1.4000	250.369			
4	1.6000	254.914			
5	1.8000	250.103			
6	2.0000	245.799			
7	2.2000	241.905			
8	2.4000	238.351			
9	2.6000	235.061			
10	2.8000	232.054	55	400.0000	32.000
11	3.0000	229.236	56	450.0000	27.860
12	3.5000	222.939	57	500.0000	24.293
13	4.0000	217.464	58	550.0000	21.197
14	4.5000	212.673	59	600.0000	18.498
15	5.0000	208.369	60	650.0000	16.136
16	5.5000	204.476	61	700.0000	14.005
17	6.0000	200.921	62	800.0000	10.647
18	6.5000	197.652	63	900.0000	8.008
19	7.0000	194.625	64	1000.0000	5.975
20	8.0000	189.170	65	1200.0000	3.236
21	9.0000	184.359	66	1400.0000	1.682
22	10.0000	180.055	67	1600.0000	.854
23	12.0000	172.658	68	1800.0000	.532
24	14.0000	166.312			
25	16.0000	160.859			
26	18.0000	155.948			
27	20.0000	151.745			
28	22.0000	147.854			
29	24.0000	144.301			
30	26.0000	141.033			
31	28.0000	138.008			
32	30.0000	135.191			
33	35.0000	128.900			
34	40.0000	123.451			
35	45.0000	118.647			
36	50.0000	114.351			
37	55.0000	110.467			
38	60.0000	106.922			
39	65.0000	103.663			
40	70.0000	100.647			
41	80.0000	95.218			
42	90.0000	90.436			
43	100.0000	86.164			
44	120.0000	78.791			
45	140.0000	72.532			
46	160.0000	67.228			
47	180.0000	62.531			
48	200.0000	58.354			
49	220.0000	54.601			
50	240.0000	51.200			
51	260.0000	48.096			
52	280.0000	45.247			
53	300.0000	42.620			
54	350.0000	36.852			

Table 3
 Predicted drawdown
 600 gpm
 2 days

DRAWDOWN # 2		gpm		Days			
T=	450.0000	S=	.0033	Q=	600.0000	TIME=	8.0000
	DISTANCE	DRAWDOWN					
1	1.0000	302.428					
2	1.2000	294.980					
3	1.4000	288.633					
4	1.6000	283.229					
5	1.8000	278.417					
6	2.0000	274.113					
7	2.2000	270.220					
8	2.4000	266.666					
9	2.6000	263.395					
10	2.8000	260.369	55	400.0000		58.354	
11	3.0000	257.550	56	450.0000		53.721	
12	3.5000	251.253	57	500.0000		49.614	
13	4.0000	245.799	58	550.0000		45.938	
14	4.5000	240.987	59	600.0000		42.620	
15	5.0000	236.683	60	650.0000		39.605	
16	5.5000	232.790	61	700.0000		36.852	
17	6.0000	229.236	62	750.0000		34.330	
18	6.5000	225.965	63	800.0000		32.000	
19	7.0000	222.939	64	1000.0000		24.293	
20	8.0000	217.484	65	1200.0000		18.498	
21	9.0000	212.673	66	1400.0000		14.065	
22	10.0000	208.369	67	1600.0000		10.647	
23	12.0000	200.921	68	1800.0000		8.008	
24	14.0000	194.625	69	2000.0000		5.975	
25	16.0000	189.176	70	2200.0000		4.419	
26	18.0000	184.359	71	2400.0000		3.236	
27	20.0000	180.055	72	2600.0000		2.345	
28	22.0000	176.162	73	2800.0000		1.682	
29	24.0000	172.608	74	3000.0000		1.197	
30	26.0000	169.339	75	3500.0000		.555	
31	28.0000	166.312					
32	30.0000	163.494			(FT)	(FT)	
33	35.0000	157.199					
34	40.0000	151.746					
35	45.0000	146.936					
36	50.0000	142.634					
37	55.0000	138.743					
38	60.0000	135.191					
39	65.0000	131.924					
40	70.0000	128.900					
41	80.0000	123.451					
42	90.0000	118.647					
43	100.0000	114.351					
44	120.0000	106.922					
45	140.0000	100.647					
MAC 2 → 46	160.0000	95.218					
47	180.0000	90.436					
48	200.0000	86.154					
49	220.0000	82.306					
50	240.0000	78.791					
51	260.0000	75.553					
52	280.0000	72.582					
MAC 1 → 53	300.0000	69.812					
54	350.0000	63.652					

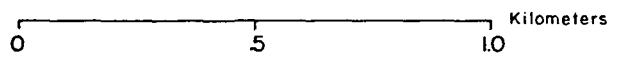
Table 4
Predicted drawdown
600 gpm
8 days

MONROE - RED HILL HEAT FLOW



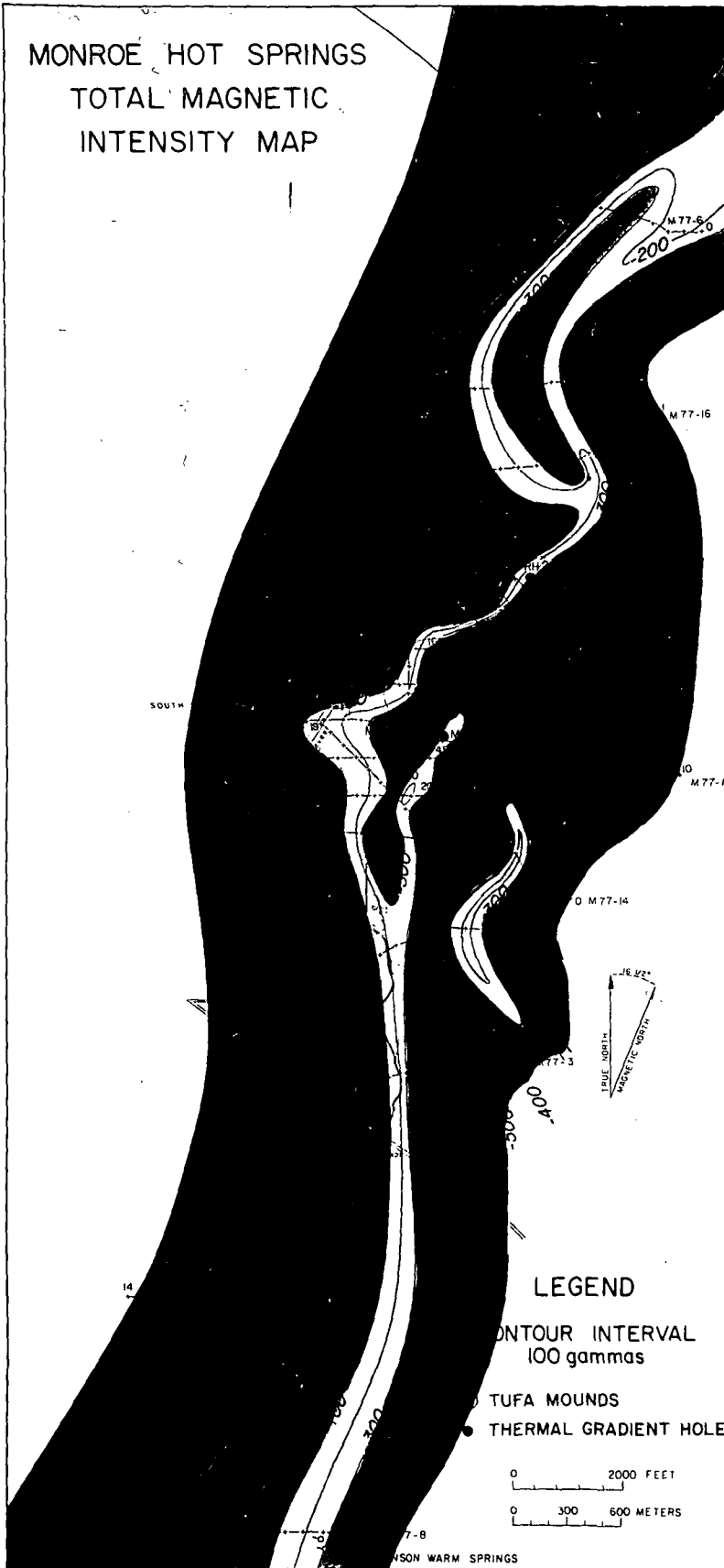
LEGEND

- Heat Flow Holes (mW m²)
- ☞ Tufo Mounds



SCALE

MONROE HOT SPRINGS
TOTAL MAGNETIC
INTENSITY MAP



LEGEND

CONTOUR INTERVAL
100 gammas

TUFA MOUNDS

THERMAL GRADIENT HOLE

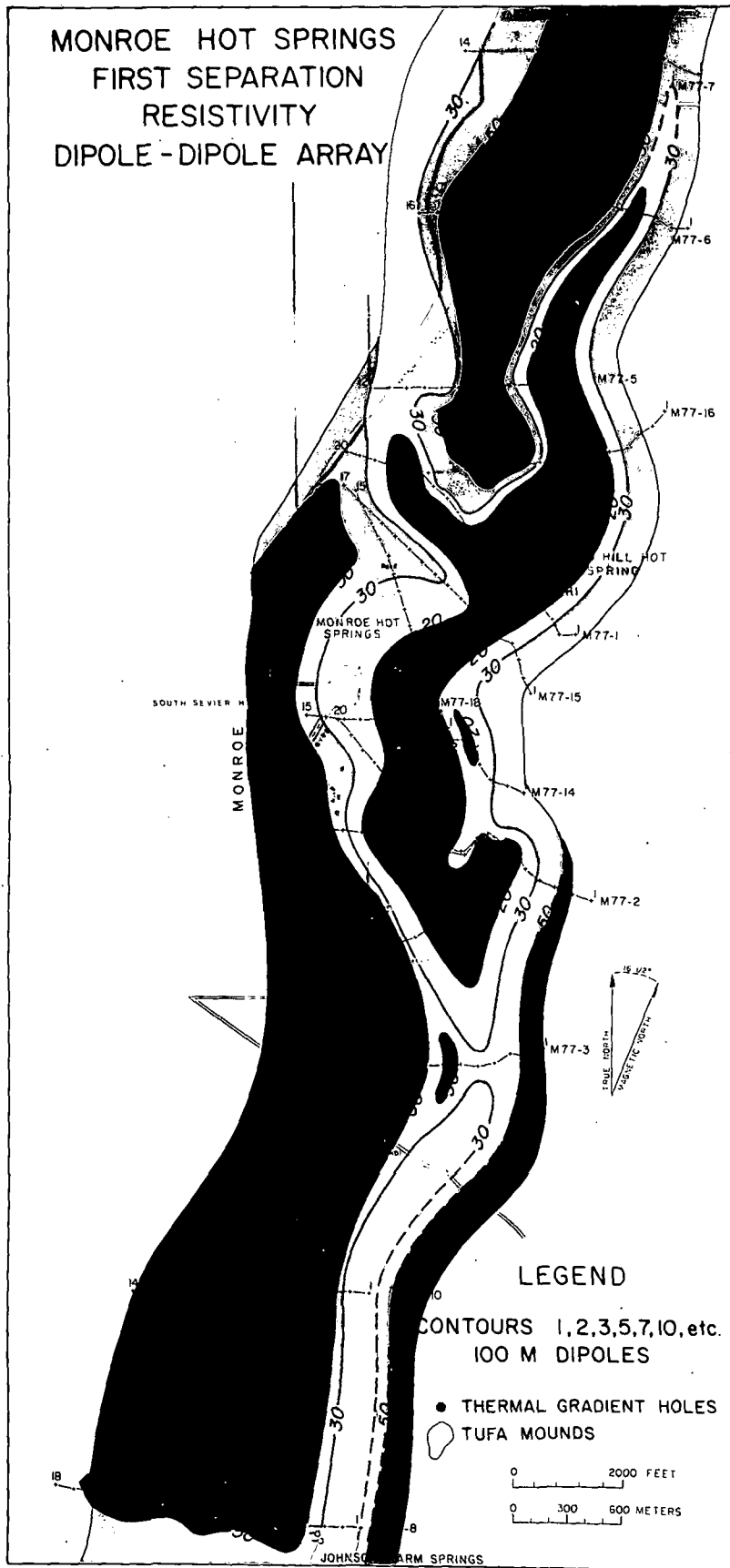
0 2000 FEET

0 300 600 METERS

M77-8

MONROE WARM SPRINGS

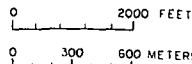
MONROE HOT SPRINGS
 FIRST SEPARATION
 RESISTIVITY
 DIPOLE - DIPOLE ARRAY



LEGEND

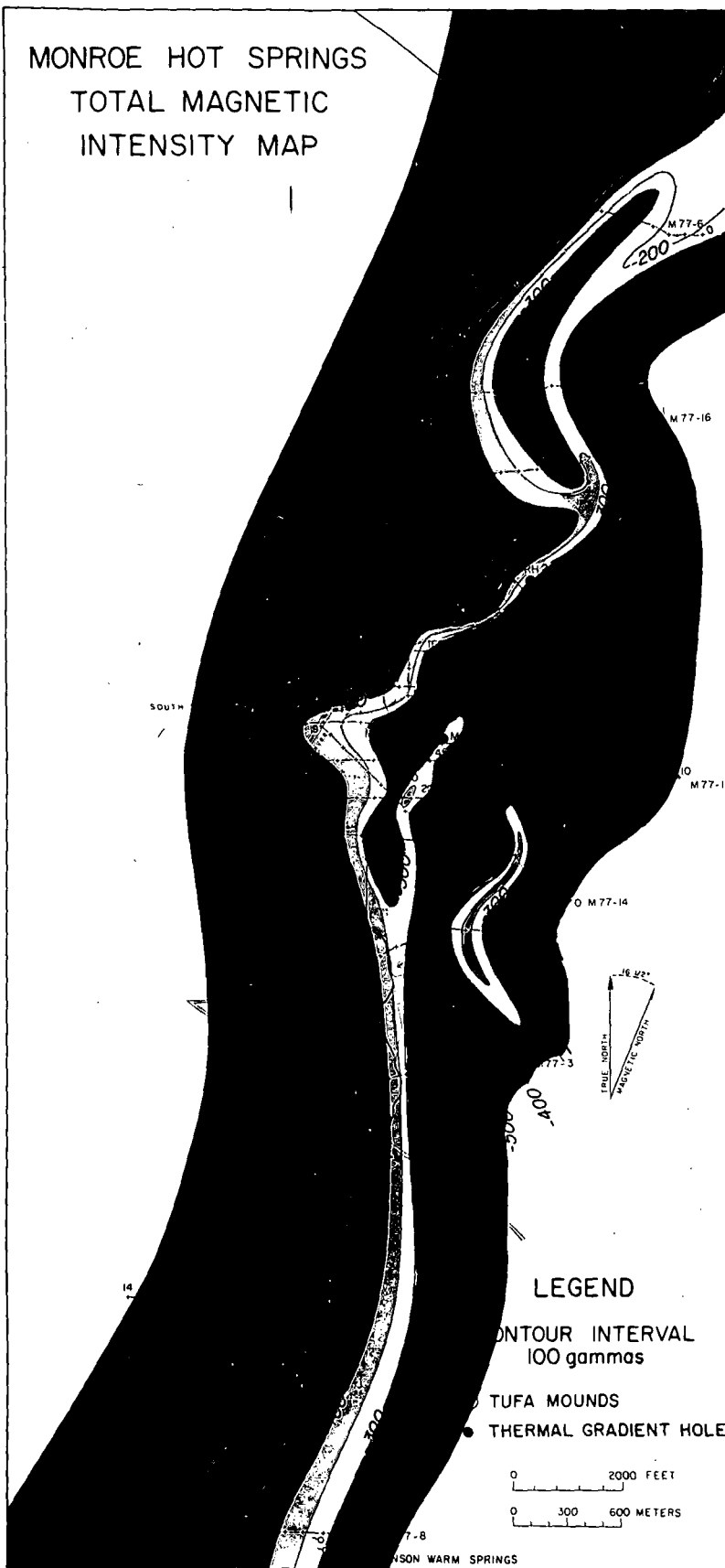
CONTOURS 1, 2, 3, 5, 7, 10, etc.
 100 M DIPOLES

- THERMAL GRADIENT HOLES
- TUFAS MOUNDS



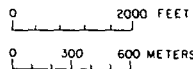
JOHNSON ARM SPRINGS

MONROE HOT SPRINGS
TOTAL MAGNETIC
INTENSITY MAP

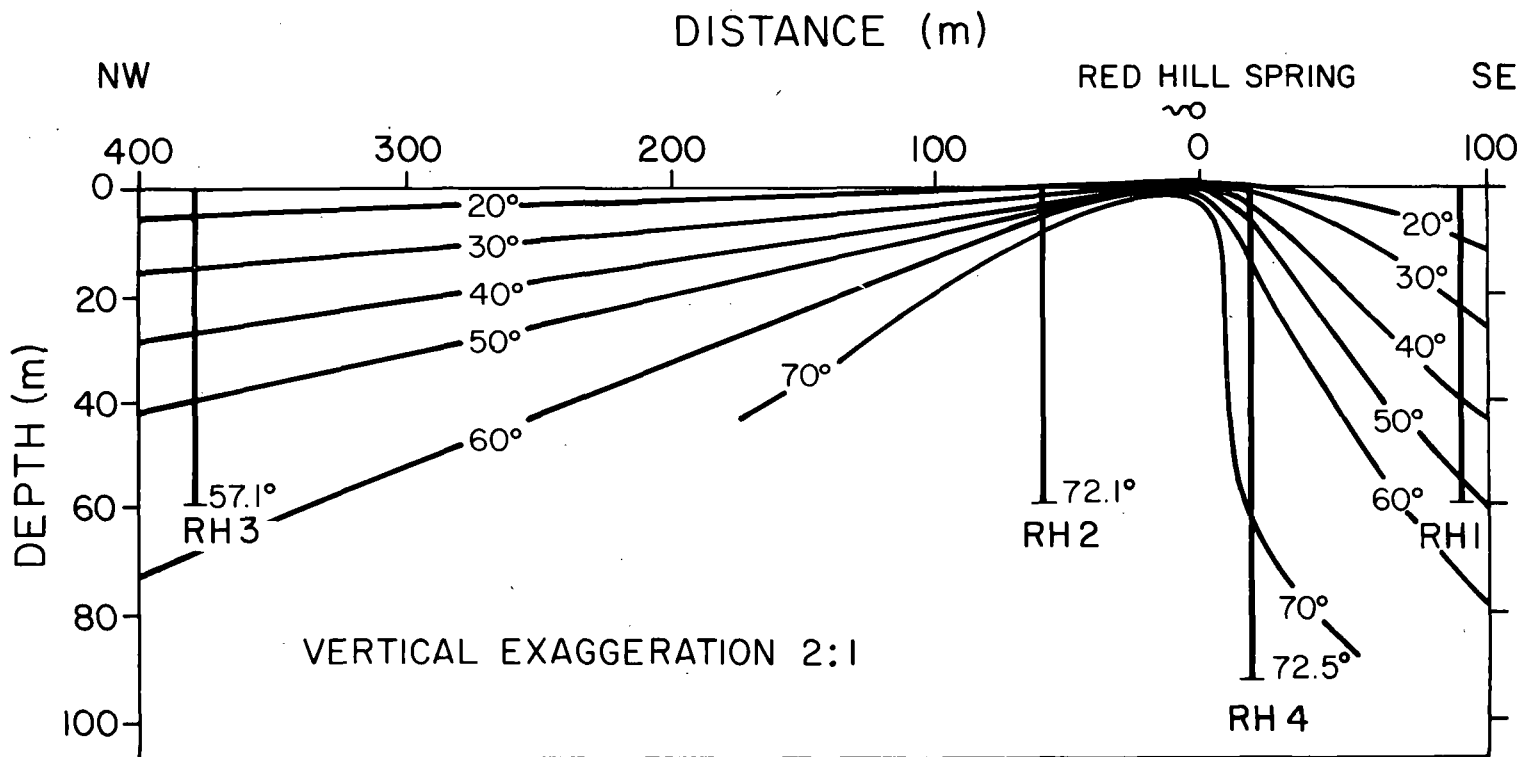
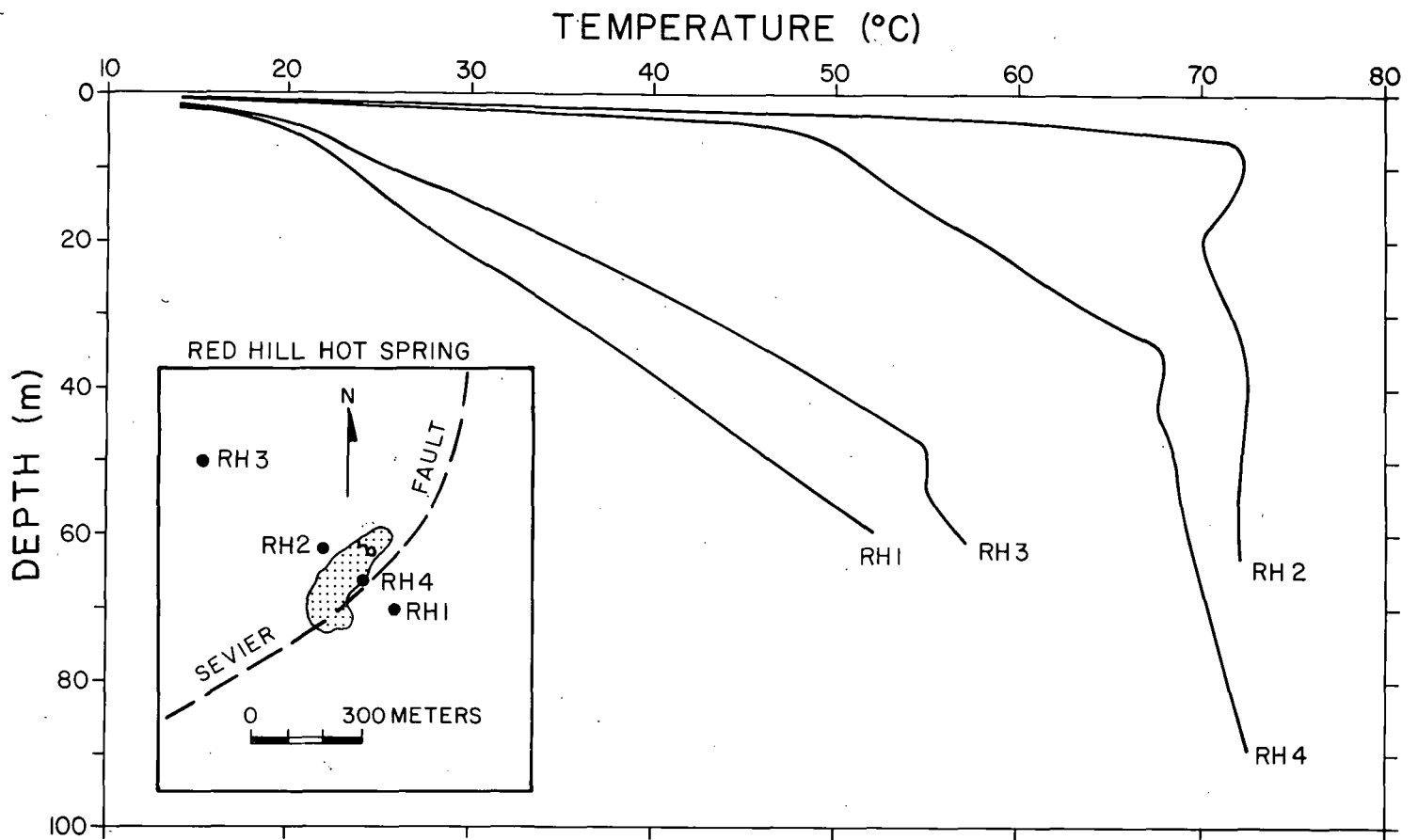


LEGEND

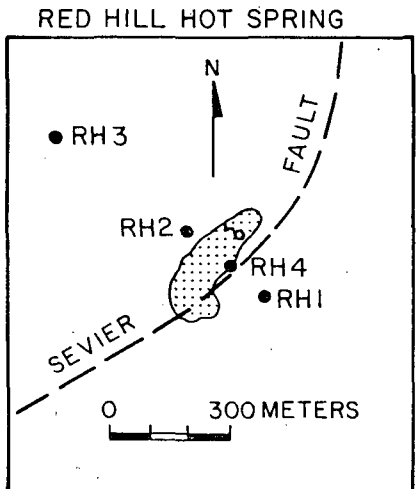
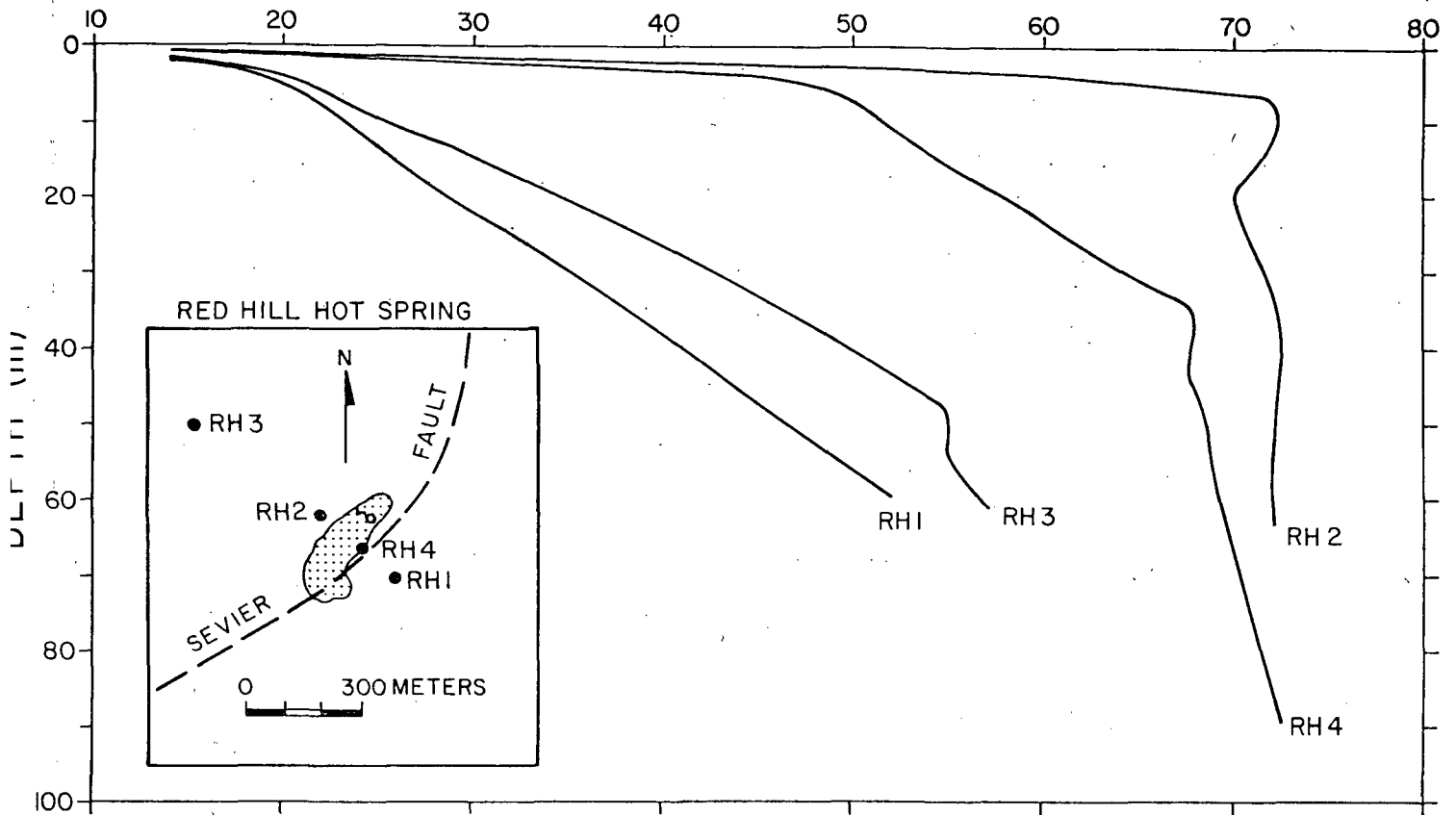
- CONTOUR INTERVAL
100 gammas
- TUFA MOUNDS
- THERMAL GRADIENT HOLE



7-8
MONROE WARM SPRINGS



TEMPERATURE (°C)



DISTANCE (m)

